

Molecular Physics

An International Journal at the Interface Between Chemistry and Physics

ISSN: (Print) (Online) Journal homepage: <https://www.tandfonline.com/loi/tmph20>

Molecular charge distributions in strong magnetic fields: a conceptual and current DFT study

Tom J. P. Irons, Bang C. Huynh, Andrew M. Teale, Frank De Proft & Paul Geerlings

To cite this article: Tom J. P. Irons, Bang C. Huynh, Andrew M. Teale, Frank De Proft & Paul Geerlings (2022): Molecular charge distributions in strong magnetic fields: a conceptual and current DFT study, Molecular Physics, DOI: [10.1080/00268976.2022.2145245](https://doi.org/10.1080/00268976.2022.2145245)

To link to this article: <https://doi.org/10.1080/00268976.2022.2145245>



© 2022 The Author(s). Published by Informa UK Limited, trading as Taylor & Francis Group



Published online: 24 Nov 2022.



Submit your article to this journal [↗](#)



Article views: 376



View related articles [↗](#)



View Crossmark data [↗](#)

Molecular charge distributions in strong magnetic fields: a conceptual and current DFT study

Tom J. P. Irons ^a, Bang C. Huynh ^a, Andrew M. Teale ^{a,b}, Frank De Proft ^c and Paul Geerlings ^c

^aSchool of Chemistry, University of Nottingham, Nottingham, UK; ^bHylleraas Centre for Quantum Molecular Sciences, Department of Chemistry, University of Oslo, Oslo, Norway; ^cResearch Group of General Chemistry (ALGC), Vrije Universiteit Brussel, Brussels, Belgium

ABSTRACT

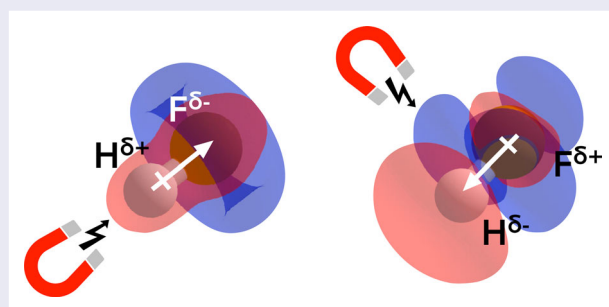
The effect of strong magnetic fields on the charge distribution of the hydrogen halides, H₂O and NH₃ is studied in the context of recent extensions of conceptual density functional theory to include additional variables such as external magnetic fields. From conceptual DFT studies on atoms in strong magnetic fields, changes in electronegativity and hardness suggest a reversal in polarity for all three diatomic molecules under these conditions. This is confirmed by current DFT calculations on these molecules in the presence of strong magnetic fields parallel and perpendicular to the internuclear axis; in the former case the electric dipole moment only undergoes small changes whereas in the latter case it changes significantly and also reverses in direction, doing so at lower field strength if the geometry is relaxed. The absence of a dipole moment induced perpendicular to the bond when a magnetic field is applied in this direction is understood by consideration of time reversal symmetry. Similar results are obtained for H₂O and NH₃; this may be an important point to consider in future studies focused on the unresolved question on the behaviour of hydrogen bonding in applied magnetic fields.

ARTICLE HISTORY

Received 10 October 2022
Accepted 3 November 2022

KEYWORDS

Conceptual density-functional theory; current-density-functional theory; strong magnetic fields; dipole moment; magnetic symmetry







1. Introduction

The effect on the properties of atoms and molecules of their environments has long been of interest in chemistry and physics. In recent years however, there has been an increasing focus on the effect of such conditions as external electric fields, [1, 2] mechanical forces [3, 4] and high pressures [5, 6] on chemical reactivity itself, leading to the new forms of chemistry that occur in these sometimes extreme conditions being of growing interest to the chemistry community. In the words of Shaik in Ref. [2], these are expected to be ‘novel effectors of chemical

change’. Often the development of experimental methods to create these reaction conditions in the laboratory has been concomitant to the development of theoretical methods to describe chemical systems under these conditions, such as the oriented external electric field method, [7] methods in the domain of mechanochemistry [8] and recent developments in the area of chemistry under very high pressure, from organic synthesis to materials design [9, 10].

The behaviour of chemical systems under strong magnetic fields has, until recently, been less widely

CONTACT Tom J. P. Irons  tom.irons@nottingham.ac.uk  School of Chemistry, University of Nottingham, University Park, Nottingham NG7 2RD, UK; Paul Geerlings  pgeerlin@vub.be  Research Group of General Chemistry (ALGC), Vrije Universiteit Brussel, Brussels, Belgium

This article was originally published with errors, which have now been corrected in the online version. Please see Correction (<http://dx.doi.org/10.1080/00268976.2022.2154030>)

investigated; the astrophysical discovery of magnetic fields on the surface of white dwarf stars much stronger than those on earth [11, 12] has motivated the development of computational methods to model atoms under such conditions in order to interpret absorption spectra observed from these bodies [13]. A large number of studies, starting in the 1990s, of the electronic structures of light atoms in strong magnetic fields followed, revealing changes in the electronic configuration of ground and excited states with increasing field strength and the concomitant distortion of their physical properties such as charge densities [14]. It was noted that, at increasing field strength, electronic configurations of higher spin projection and orbital angular momentum become the ground state; eventually fully spin-polarised configurations become the ground state, as shown for example in the study by Ivanov and Schmelcher on the carbon atom computed at the Hartree–Fock level with fields ranging from 0 to 2.23×10^9 T [15]. These studies and others, see for example Ref. [16] and references therein, inspired a recent study by the present authors into the evolution of conceptual density functional theory [17–23] descriptors in the presence of strong magnetic fields [24]. This extension to conceptual density functional theory follows recent work to include the effect of temperature, [25, 26] external electric fields, [27] mechanical forces, [28, 29] confinement [30, 31] and applied pressure [32].

Whilst there has been extensive study of atoms in strong magnetic fields, comparatively little is known concerning the behaviour of molecules and solid-state systems under these conditions. The computational modelling of general systems under these conditions, in which finite basis set techniques must be adapted with orbitals becoming complex, is significantly more complicated and computationally costly than at zero field. These studies were extended to the H_2 molecule in parallel and perpendicular magnetic fields [33–35] and, more recently, other diatomic molecules in the work of Lehtola, [36] reporting fully numerical calculations on low lying electronic states of H_2 , HeH^+ , LiH , BeH^+ , BH and CH^+ as a function of the field strength parallel to the molecular axis.

The development of the LONDON electronic structure code [37] by Tellgren *et al.* [38] permitted non-perturbative calculations of general molecular systems in magnetic fields of arbitrary strength by using a basis of London atomic orbitals [39]. Extending these techniques to full configuration interaction theory, Lange *et al.* [40] revealed a new bonding mechanism in H_2 under very strong magnetic fields, which when oriented perpendicular to the bond results in the triplet state becoming bound and more stable than the singlet state; this phenomenon was termed ‘perpendicular paramagnetic bonding’. Subsequent work, with the adaptation of other electronic

structure methods to systems in strong magnetic fields in LONDON and in other electronic structure packages, including TURBOMOLE, [41] QCUMBRE, [42] BAGEL [43] and the QUEST code used in the present work, [44] has significantly broadened the range of chemistry that can be investigated under these extreme conditions. Recent studies have considered the effects of strong magnetic fields on the absorption spectra, [45] equilibrium geometries [46] and excitation energies [47] of atoms and molecules and the interaction energy of large molecular clusters [48] under these conditions. The work by Deb and colleagues has concentrated on electron dynamics in small atoms and molecules under the influence of strong oscillating magnetic fields using a fundamentally different quantum field density functional theory approach, details of which may be found in Ref. [49] and references therein.

One important property of chemical significance, namely the change in the charge distribution of molecules with increasing magnetic field strength, does not feature in the literature on this topic to the best of our knowledge. However the charge distribution and therefore the polarity of molecular systems are fundamental determinants of their chemical behaviour and understanding the evolution of these with magnetic field strength could be considered a requisite to developing an understanding of chemical reactivity under these conditions.

Furthermore, the changes in charge distribution in magnetic fields may provide new insight into the ongoing investigations on the effect of magnetic fields on hydrogen bonding. In the literature, which mainly considers the case for hydrogen bonding in water, experimental studies on liquid water concentrate exclusively on the macroscopic manifestations of varying hydrogen bond strength: refractive index, surface tension and viscosity, often linking measured changes in these to variations in the strength of the hydrogen bond network [50–52]. Theoretical studies on the dynamics of liquid water [53] or on the properties of the water dimer in magnetic fields [54] have investigated the link between these phenomena and hydrogen bonding but present a somewhat mixed picture. A recent study by Speake *et al.* on the behaviour of large water clusters in magnetic fields confirms the increase in interaction energy with field strength, however analysis of the accompanying change in charge density does not suggest increased strength of hydrogen bonding as the predominant reason for this [48]. It is apparent that further study will be necessary to better understand the changes in the properties of water that are observed when a magnetic field is applied [55].

It is notable that the picture is clearer in the case of an applied electric field, for which the analysis is considered at the microscopic level. For example, the quantum

chemical studies by Ramos *et al.* [56] on hydrogen bonding between hydrogen halides and HCN or NH₃ and the study by Suresh *et al.* [57] on the hydrogen bond network of water in electric fields. In Ref. [56] it was reported that a monotonic increase of the molecular dipole moments with increasing field strength was essential for understanding the changes in the hydrogen bonding network under these conditions.

Given the developments in computational methods for modelling molecular systems in strong magnetic fields and the recent work of the present authors on the evolution of atomic reactivity indicators with magnetic field strength, [24] the corollary is a subsequent study of the evolution of charge distribution in simple molecules with increasing magnetic field strength. This would be a proof-of-concept investigation and a first step to developing further insights into possible changes to chemistry in strong magnetic fields. For this purpose, the series of hydrogen halides serve as a useful basis for this study; the effects of applied electric fields to these molecules has already been studied by Ramos *et al.* [56], whilst their strong permanent dipole moments at zero field largely characterises their properties. Furthermore, it was reported in Ref. [24] that the change in reactivity descriptors with magnetic field strength appears to follow a periodic trend with elements in the same groups of the periodic table often showing a similar trend with magnetic field strength; investigation of the hydrogen halides will allow the extent to which this pattern carries over to molecules containing these atoms to be examined.

An additional finding of Ref. [24] was that the electronegativity of hydrogen, evaluated using Mulliken's expression, [58] became greater than that for each of the halogen atoms at some magnetic field strength. This would suggest that, taking a simple approximation in which the polarity of a diatomic molecule is determined only by the relative electronegativity of the constituent atoms, the bond polarity would be seen to reverse at certain magnetic field strengths. The charge transfer in such an approximation may be quantified via Huheey's equation, [59–61] and be compared with the results of dipole moment calculations for these molecules themselves in strong magnetic fields, allowing the utility of this conceptual density functional theory approach to predicting molecular properties in strong magnetic fields to be assessed. Additional study on the polarity and charge distribution of H₂O and NH₃ in magnetic fields would provide an initial insight from this perspective into the influence of magnetic field strength on the hydrogen bonding in systems of these molecules – an investigation that will be developed in forthcoming studies on molecular dimers and with the analysis of additional

descriptors such as the non-covalent interaction (NCI) descriptor [62].

The present paper henceforth is organised as follows: in Section 2 an overview of the theoretical background to conceptual density functional theory and the computational modelling of systems in strong magnetic fields is presented. In Section 3.1 the evolution of dipole moment and Mulliken charges in the hydrogen halides with increasing magnetic field strength applied parallel and perpendicular to the internuclear axis is compared with, firstly the corresponding case for applied electric fields, then the changes that would be predicted from the changes to atomic reactivity indicators with field strength. The changes in charge distribution in H₂O and NH₃ with magnetic field strength are presented in Section 3.2 together with some initial thoughts on the influence of magnetic fields on hydrogen bonding. Finally conclusions are established in Section 4 along with an outlook for future investigations.

2. Theory and computational details

2.1. Conceptual DFT

The starting point of conceptual DFT is the energy of an electronic system E expressed as a functional of the number of electrons N and the external potential v due to the atomic nuclei. Perturbations of N and v represent the changes that would occur at the onset of chemical reaction, thus the response of the energy to these perturbations connects directly to the chemical concept of reactivity [17–23].

The functional Taylor expansion of the energy functional $E(N, v)$ is given by

$$\begin{aligned} \Delta E &= \left(\frac{\partial E}{\partial N} \right)_v \Delta N + \int \left(\frac{\delta E}{\delta v(\mathbf{r})} \right)_N \Delta v(\mathbf{r}) \, d\mathbf{r} + \dots \\ &= \mu \Delta N + \int \rho(\mathbf{r}) \Delta v(\mathbf{r}) \, d\mathbf{r} + \dots, \end{aligned} \quad (1)$$

the coefficients of the derivatives, quantifying the response of the energy to a given perturbation, can be constructed in general as mixed partial and functional derivatives of the energy with respect to the particle number and external potential, respectively. In recent work the dependence of the energy on additional variables has been considered, introducing derivatives with respect to external electric fields, magnetic fields, mechanical forces, confinement and pressure [24, 27–32].

In the present work, only the first and second derivatives of the energy with respect to particle number, at fixed external potential, are required. The first of these,

the electronic chemical potential [63]

$$\mu = \left(\frac{\partial E}{\partial N} \right)_v \quad (2)$$

has been shown by Parr to be equal (up to a sign) to the Iczkowski–Margrave definition [64] of the electronegativity χ , which when evaluated by finite difference approximation, reduces to Mulliken's electronegativity expression [58]

$$\mu = -\chi = -\frac{1}{2}(I + A) \quad (3)$$

where I and A denote the first vertical ionisation potential and electron affinity, respectively. The second derivative of the energy with respect to particle number can be identified with Pearson's chemical hardness η [65, 66]

$$\eta = \left(\frac{\partial^2 E}{\partial N^2} \right)_v, \quad (4)$$

which may be approximated by the finite difference approach as the difference between I and A ,

$$\eta = \frac{1}{2}(I - A). \quad (5)$$

An extensive literature is available on the use of these and other response functions such as the Fukui function [67]

$$f(\mathbf{r}) = \left(\frac{\delta^2 E}{\delta v(\mathbf{r}) \delta N} \right) \quad (6)$$

and the linear response function [17, 68]

$$\chi(\mathbf{r}, \mathbf{r}') = \left(\frac{\delta^2 E}{\delta v(\mathbf{r}) \delta v(\mathbf{r}')} \right)_N \quad (7)$$

in a variety of studies in diverse areas of chemistry. The electron density itself belongs to this series of response functions, since $\rho(\mathbf{r}) = (\delta E / \delta v(\mathbf{r}))_N$ [17, 20]. These response properties may be used to infer chemical properties of systems on their own, or in the context of principles such as the electronegativity equalisation principle (EEP), [69, 70] the hard and soft acids and bases (HSAB) principle [66] and the maximum hardness principle (MHP) [71].

The present study makes use of Sanderson's electronegativity equalisation principle, [69, 70] which states that, upon molecule formation, the electronegativities of the constituent atoms in a molecule become equal even if the electronegativities of the atoms in isolation are different. This situation is comparable with the equalisation of (macroscopic) chemical potentials of reactants, upon which a chemical reaction equilibrium has been reached. It can readily be seen that, neglecting changes to the external potential and truncating the series expansion to second order, the change in the number of electrons ΔN for a given atom A in a diatomic molecule, relative to the

atom in isolation, can be written as [17, 59–61]

$$\Delta N_A = \frac{\chi_A - \chi_B}{2(\eta_A + \eta_B)} \quad (8)$$

where clearly ΔN_B is equal to $-\Delta N_A$. The concomitant energy change associated with the charge transfer is given by

$$\Delta E = -\frac{(\chi_A - \chi_B)^2}{4(\eta_A + \eta_B)}. \quad (9)$$

The direction of charge transfer is thereby governed by the difference in electronegativities, but its magnitude involves a modulation by the sum of their hardness. In the preceding study, [24] the electronegativity and hardness of atoms was evaluated as a function of magnetic field strength $|\mathbf{B}|$ by combining the ionisation energy and electron affinity at finite field strengths using field-dependent forms of Equations (3) and (5),

$$\begin{aligned} \chi(\mathbf{B}) &= \frac{1}{2}(I(\mathbf{B}) + A(\mathbf{B})) \\ \eta(\mathbf{B}) &= \frac{1}{2}(I(\mathbf{B}) - A(\mathbf{B})) \end{aligned} \quad (10)$$

It was shown that the ground-state electronic configurations of the neutral atoms, anions and cations change frequently with increasing magnetic field strength, leading to remarkable changes in the periodic table of electronegativity and hardness at strong fields with $|\mathbf{B}| \geq 0.5B_0$ compared to the zero-field case [24].

The data at such high fields will be used to gain an initial, approximate insight into the change in the charge distribution under these conditions compared to the absence of a field by inserting them in the Huheey equation, Equation (8), which may be written in its \mathbf{B} dependent form as

$$\Delta N_A(\mathbf{B}) = \frac{\chi_A(\mathbf{B}) - \chi_B(\mathbf{B})}{2(\eta_A(\mathbf{B}) + \eta_B(\mathbf{B}))}. \quad (11)$$

2.2. Systems in strong fields

To study the properties of atoms and molecules in magnetic fields of the order of $1B_0 = \hbar e^{-1} a_0^{-2} = 2.3505 \times 10^5$ T, it is necessary to consider the effects of the magnetic field in a non-perturbative manner. In the presence of a uniform external magnetic field \mathbf{B} , the non-relativistic electronic Hamiltonian is given in atomic units by

$$\begin{aligned} \hat{\mathcal{H}} &= \hat{\mathcal{H}}_0 + \frac{1}{2}(\mathbf{B} \times \mathbf{r}_0) \cdot \hat{\mathbf{p}} + \mathbf{B} \cdot \hat{\mathbf{s}} \\ &+ \frac{1}{8}(\mathbf{B} \times \mathbf{r}_0) \cdot (\mathbf{B} \times \mathbf{r}_0), \end{aligned} \quad (12)$$

with $\hat{\mathbf{p}}$ the canonical momentum operator, $\hat{\mathbf{s}}$ the spin operator, \mathbf{r}_0 the position \mathbf{r} relative to some gauge-origin

\mathbf{O} ($\mathbf{r}_0 = \mathbf{r} - \mathbf{O}$) and $\hat{\mathcal{H}}_0$ the Hamiltonian at zero-field. The position of the gauge-origin may be related to the magnetic field through a magnetic vector potential \mathbf{A} , defined in the Coulomb gauge for which $\nabla \cdot \mathbf{A} = 0$ as

$$\mathbf{A}_0(\mathbf{r}) = \frac{1}{2} \mathbf{B} \times (\mathbf{r} - \mathbf{O}). \quad (13)$$

A translation of the gauge-origin $\mathbf{O} \rightarrow \mathbf{O}'$ transforms the vector potential as

$$\mathbf{A}_{\mathbf{O}'}(\mathbf{r}) = \mathbf{A}_0(\mathbf{r}) - \nabla \mathbf{A}_0(\mathbf{O}') \cdot \mathbf{r}, \quad (14)$$

which implies a unitary transformation of the Hamiltonian and a compensating transformation of the eigenfunctions Ψ , respectively, given by

$$\hat{\mathcal{H}}' = e^{i\mathbf{A}_0(\mathbf{O}') \cdot \mathbf{r}} \hat{\mathcal{H}} e^{-i\mathbf{A}_0(\mathbf{O}') \cdot \mathbf{r}}, \quad \Psi' = e^{i\mathbf{A}_0(\mathbf{O}') \cdot \mathbf{r}} \Psi, \quad (15)$$

which results in the gauge-origin invariance of the system observables such as its energy and the charge density. The gauge-origin dependence of the wavefunction implied in Equation (15) is not however reproducible in a finite basis of, for example, Gaussian functions. A modification of the basis functions such that they themselves explicitly include the gauge-origin dependence however corrects this deficiency; London atomic orbitals (LAOs) ω are constructed as the product of standard Gaussian functions φ and a gauge-origin dependent phase factor, [39, 72]

$$\omega_a(\mathbf{r}) = \varphi_a(\mathbf{r}) e^{-\frac{i}{2} \mathbf{B} \times (\mathbf{R}_a - \mathbf{O}) \cdot \mathbf{r}}, \quad (16)$$

where \mathbf{R}_a is the position at which the orbital ω_a is centred. The use of LAOs as basis functions results in wavefunctions that show the correct behaviour, to first order, with respect to the magnetic field whilst the observables remain gauge-origin invariant, thus permitting electronic systems to be modelled in the presence of arbitrary strength magnetic fields beyond the perturbative regime [38].

The use of LAOs in electronic structure calculations requires the adaptation of conventional zero-field implementations, since the basis functions and wavefunction can no longer be assumed to be real. For many *ab initio* electronic structure methods, the implementations can be generalised to the use of LAOs without changes to the theories themselves by ensuring complex-conjugate symmetries are properly respected and molecular integral algorithms are adapted for complex basis functions [73]. Such implementations have been developed for Hartree-Fock (HF), [38, 74] configuration interaction, [40] Møller-Plesset, coupled-cluster [75] and equation of motion coupled cluster theories [76] and current density functional theory (current DFT) [77, 78].

The treatment of molecular systems in strong electric fields is somewhat simpler since, given a uniform static electric field \mathcal{E} , the non-relativistic electronic Hamiltonian contains only one term linear in the field [79, 80]

$$\hat{\mathcal{H}} = \hat{\mathcal{H}}_0 - \mathcal{E} \cdot \mathbf{r}, \quad (17)$$

where the electric field is given in atomic units $1 \text{ a.u.} = m^2 e^5 \hbar^{-4} = 5.1422 \times 10^{11} \text{ Vm}^{-1}$. Treating the electric field in a non-perturbative way through its direct inclusion in the Hamiltonian allows its contribution to the energy to be written as the dot product of the electric field and the electric dipole moment of the molecule.

2.3. Current density functional theory

In contrast to *ab initio* methods, the adaptation of DFT to systems in the presence of strong magnetic fields requires more significant changes since, due to the additional field-dependent terms in the Hamiltonian of Equation (12), electronic systems are not possible to fully describe exclusively with the charge density as in the case of zero-field DFT. The density functional becomes dependent on an additional term; in the case of magnetic field DFT the dependence is on the magnetic field explicitly [81, 82] whilst in the case of current DFT the dependence is on the magnetically induced current density [77, 78].

In this work, the Vignale-Rasolt formulation of current DFT is utilised, with the universal density functional \mathcal{F} depending on the charge and paramagnetic current densities (ρ, \mathbf{j}_p) and energy E depending on the scalar and vector potentials (v, \mathbf{A}). A convex-conjugate formalism of current DFT analogous to that of Lieb [83] may be obtained by defining an energy functional $\mathcal{E}(u, \mathbf{A})$ depending on a modified scalar potential $u = v + \frac{1}{2} \mathbf{A}^2$ in which it is concave and related to $\mathcal{F}(\rho, \mathbf{j}_p)$ by convex conjugation as [78, 84]

$$\mathcal{E}(u, \mathbf{A}) = \inf_{\rho, \mathbf{j}_p} \left\{ \mathcal{F}(\rho, \mathbf{j}_p) + \int u(\mathbf{r}) \rho(\mathbf{r}) \, \text{d}\mathbf{r} + \int \mathbf{A}(\mathbf{r}) \cdot \mathbf{j}_p(\mathbf{r}) \, \text{d}\mathbf{r} \right\}, \quad (18)$$

$$\mathcal{F}(\rho, \mathbf{j}_p) = \sup_{u, \mathbf{A}} \left\{ \mathcal{E}(u, \mathbf{A}) - \int u(\mathbf{r}) \rho(\mathbf{r}) \, \text{d}\mathbf{r} - \int \mathbf{A}(\mathbf{r}) \cdot \mathbf{j}_p(\mathbf{r}) \, \text{d}\mathbf{r} \right\}. \quad (19)$$

The functional $\mathcal{F}(\rho, \mathbf{j}_p)$ may be written as a sum of individual terms according to the Kohn-Sham (KS) approach as [85, 86]

$$\mathcal{F}(\rho, \mathbf{j}_p) = \mathcal{I}_s(\rho, \mathbf{j}_p) + J(\rho) + \mathcal{E}_{\text{xc}}(\rho, \mathbf{j}_p), \quad (20)$$

where $\mathcal{T}_s(\rho, \mathbf{j}_p)$ is the non-interacting kinetic energy, $J(\rho)$ the classical Coulomb energy and $\mathcal{E}_{xc}(\rho, \mathbf{j}_p)$ the exchange-correlation energy. The one-particle KS equations for current DFT follow from this as

$$\left[\frac{1}{2} \hat{p}^2 + \frac{1}{2} \{ \hat{\mathbf{p}}, \mathbf{A}_s \} + u_s + \hat{\mathbf{s}} \cdot (\nabla \times \mathbf{A}_s) \right] \phi_p = \varepsilon_p \phi_p, \quad (21)$$

solutions of which give the KS orbitals ϕ_p and corresponding orbital energies ε_p . The charge and paramagnetic current densities of the non-interacting system, given respectively by

$$\rho = \sum_{\sigma} \sum_i^{\text{occ}} \phi_{i\sigma}^* \phi_{i\sigma} \quad (22)$$

$$\mathbf{j}_p = -\frac{i}{2} \sum_{\sigma} \sum_i^{\text{occ}} [\nabla(\phi_{i\sigma}) \phi_{i\sigma}^* - \phi_{i\sigma} (\nabla \phi_{i\sigma})^*] \quad (23)$$

reproduce the respective quantities of the physically interacting system, whilst the KS scalar and vector potentials are respectively defined as

$$u_s = v_{\text{ext}} + \frac{1}{2} \mathbf{A}_s^2 + v_J + v_{\text{xc}}, \quad \mathbf{A}_s = \mathbf{A}_{\text{ext}} + \mathbf{A}_{\text{xc}} \quad (24)$$

where v_{xc} and \mathbf{A}_{ext} are the external potentials arising due to the nuclei and external magnetic field, respectively, v_J the Coulomb potential and the exchange-correlation potentials are defined as

$$v_{\text{xc}} = \frac{\delta \mathcal{E}(\rho, \mathbf{j}_p)}{\delta \rho}, \quad \mathbf{A}_{\text{xc}} = \frac{\delta \mathcal{E}(\rho, \mathbf{j}_p)}{\delta \mathbf{j}_p}. \quad (25)$$

It has been shown that meta-generalised gradient approximations (mGGAs) to the exchange-correlation energy depending on the non-interacting kinetic energy density τ , in particular that of Tao–Perdew–Staroverov–Scuseria (TPSS), [87] can remain reliably accurate for calculations in strong magnetic fields [88]. To ensure the exchange-correlation functional remains gauge-origin invariant, a modified kinetic energy density of the form

$$\tilde{\tau}_{\sigma} = \sum_i^{\text{occ}} (\nabla \phi_{i\sigma})^* \cdot (\nabla \phi_{i\sigma}) - \frac{|\mathbf{j}_{p\sigma}|^2}{\rho_{\sigma}} = \tau_{\sigma} - \frac{|\mathbf{j}_{p\sigma}|^2}{\rho_{\sigma}} \quad (26)$$

proposed by Dobson [89] and Becke [90] is employed; this may be substituted into the TPSS functional to yield a current DFT form, denoted cTPSS, [91] which is used throughout this work.

2.4. Computational details

All calculations have been carried out using current DFT with the cTPSS functional, described in Section 2.3, in

the uncontracted aug-cc-pVQZ basis set [92, 93] and employing the resolution of the identity approximation with the AUTOAUX auxiliary basis [94].

For calculations in the presence of an external electric field, the OEFF approach [2] was employed with field strengths of $|\mathcal{E}| = 0.0 - 0.1$ a.u. with the field vector in the direction of increasing Cartesian coordinates and electric dipole moment calculated for molecule with electronic charge density ρ and N nuclei of charge Z_I and position \mathbf{R}_I as

$$\boldsymbol{\mu}_e = \sum_I^N Z_I \mathbf{R}_I - \int \mathbf{r} \rho(\mathbf{r}) \, d\mathbf{r}. \quad (27)$$

All calculations have been undertaken using the QUEST code [44]. Unless stated otherwise all quantities are quoted in atomic units where, for magnetic fields $1B_0 = \hbar e^{-1} a_0^{-2} = 2.3505 \times 10^5$ T and for electric fields 1 a.u. = $m^2 e^5 \hbar^{-4} = 5.1422 \times 10^{11}$ Vm⁻¹.

3. Results and discussion

In this section, the dipole moments of a set of small molecules in the presence of strong external electric and magnetic fields are presented. The observed trends are compared with those that may be predicted from the chemical descriptors of atoms under these conditions and rationalised, where appropriate, using Mulliken atomic charges [95]. Furthermore, the effect on these results of relaxing the geometry at increasing magnetic field strengths is considered.

3.1. Hydrogen halides

To examine the relationship between molecular properties in the presence of fields and those which would be predicted from the chemical reactivity indicators of their constituent atoms, the series of hydrogen halides HF, HCl and HBr are studied here.

Considering first the chemical reactivity indicators of the atoms, the electronegativity and hardness values of the constituent atoms in HF, HCl and HBr previously presented in Ref. [24] are given in Table 1 at magnetic field strengths of $|\mathbf{B}| = 0, 0.2, 0.5$ and $1.0B_0$. As described previously, the values of electronegativity and hardness for each species with respect to increasing magnetic field strength show a piecewise behaviour, in which changes to the ground state electronic configuration of the atoms and their respective anions and cations results in distinct segments in the values of χ and η with respect to $|\mathbf{B}|$ [24].

It was shown in Ref. [24] that the ground-state configuration for each of H, F, Cl and Br remains unchanged in the range $|\mathbf{B}| = 0.0 - 0.2B_0$, making it instructive

Table 1. Difference in electronegativity values ($\Delta\chi = \chi_H - \chi_X$) in E_h , sum of hardness values ($\sum \eta$) in E_h and change in number of electrons ($\Delta N = N_H - N_X$) for the hydrogen halides HF, HCl and HBr as a function of the magnetic field strength $|\mathbf{B}| / B_0$.

	$ \mathbf{B} / B_0$	0.0	0.2	0.5	1.0
HF	$\Delta\chi$	-0.127	+0.042	+0.195	+0.210
	$\sum \eta$	+0.489	+0.581	+0.519	+0.622
	ΔN	-0.130	+0.036	+0.188	+0.169
HCl	$\Delta\chi$	-0.042	+0.104	+0.144	+0.150
	$\sum \eta$	+0.405	+0.466	+0.517	+0.558
	ΔN	-0.052	+0.112	+0.144	+0.135
HBr	$\Delta\chi$	-0.018	+0.122	+0.136	+0.179
	$\sum \eta$	+0.390	+0.438	+0.474	+0.553
	ΔN	-0.023	+0.139	+0.144	+0.161

to compare between the charge transfer predicted by Equation (11) at zero field and $0.2B_0$. It was noted in Ref. [24] that at $|\mathbf{B}| = 0.5B_0$, the electronegativity of H had become greater than that of F, Cl and Br – a reversal of the case at zero field; as such this field strength is also considered in Table 1, as is the highest field strength $|\mathbf{B}| = 1.0B_0$ for comparison. Over this range of $|\mathbf{B}|$, the ground state electronic configuration of H was shown to remain unchanged, whilst that of F undergoes one change at $|\mathbf{B}| = 0.6B_0$ and those of both Cl and Br undergo three changes at $|\mathbf{B}| = 0.3, 0.5$ and $0.7B_0$ [24].

The ground-state energies of these four atoms as a function of magnetic field strength over the range relevant for the subsequent discussion of their respective molecules are shown in Figure 1.

In the absence of a field, the values of ΔN shown in Table 1 are in line with what conventional chemical intuition would predict – namely that, since the halogen atoms are more electronegative than hydrogen, in the hydrogen halides there should be a charge transfer from hydrogen to the halogen and thus a negative value of ΔN . Since the halogens become less electronegative going down the group from $F \rightarrow Cl \rightarrow Br$, the magnitude of ΔN should decrease from $HF \rightarrow HCl \rightarrow HBr$. However it can be seen in Table 1 that at $|\mathbf{B}| = 0.2B_0$, with the atomic ground-state configurations unchanged from at zero field, ΔN is positive for all three molecules, implying a charge transfer *from* the halogen *to* hydrogen. This reversal of the zero-field case follows from the change in relative electronegativities that occurs, with hydrogen becoming more electronegative than each of the halogens; this can be seen in the Supporting Information of Ref. [24] and is plotted here for hydrogen and the three halogens in Figure 2.

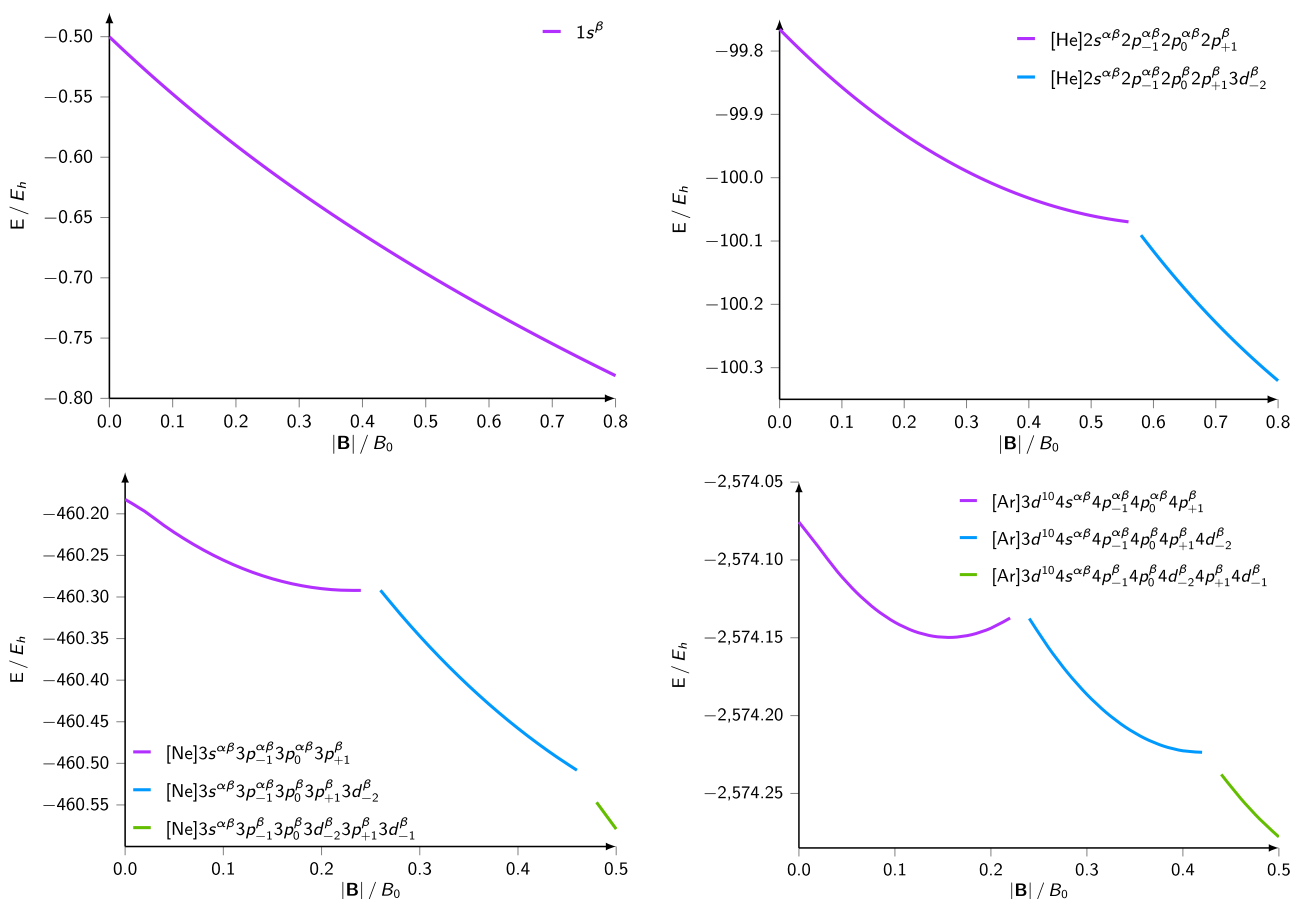


Figure 1. Ground state energies in E_h and electronic configurations of H (upper left), F (upper right), Cl (lower left) and Br (lower right) as a function of magnetic field strength, calculated with current DFT using the cTPSS functional.

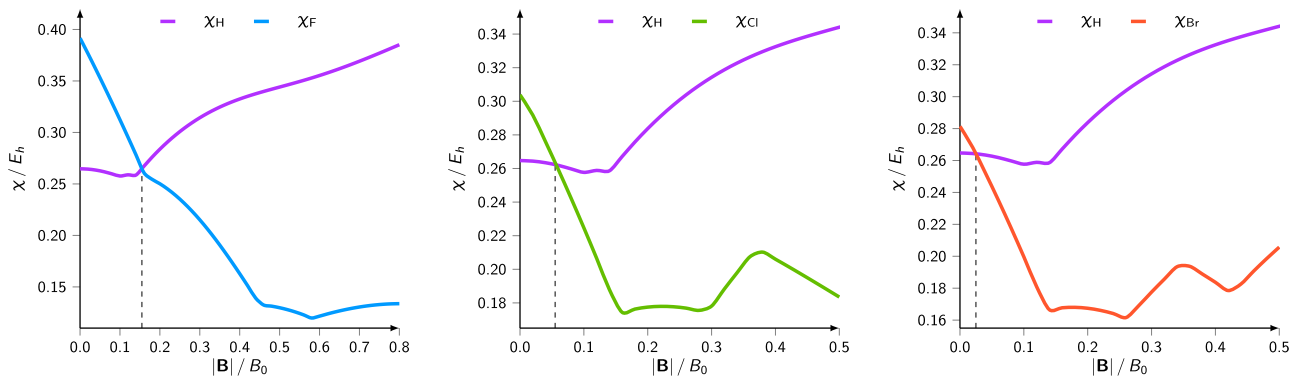


Figure 2. The electronegativities of H and F (left), Cl (centre) and Br (right) plotted as a function of magnetic field strength, with the crossing points indicated in each case.

It can be seen in Figure 2 that the magnetic field strength at which χ_H becomes greater than χ_X decreases for $X = \text{F} \rightarrow \text{Cl} \rightarrow \text{Br}$, occurring at $|\mathbf{B}| = 0.16, 0.05$ and $0.03B_0$, respectively. Since χ_H does not change significantly up to $|\mathbf{B}| = 0.16B_0$, these differences are determined entirely by the behaviour of χ_X with $|\mathbf{B}|$, all of which decrease by a comparable value in this range. The difference in zero-field electronegativity between the two atoms however decreases from $\text{F} \rightarrow \text{Cl} \rightarrow \text{Br}$, implying a decreasing zero-field bond polarity in the respective hydrogen halide; it follows that the larger the zero-field bond polarity, the greater the field strength required to reverse its direction. The difference in electronegativity and the sum of hardness values for the hydrogen halides shown in Table 1 generally continue to increase with increasing field strength, with ΔN appearing to exhibit smaller changes at higher field strengths (with comparatively small decreases for HF and HCl and a comparatively small increase for HBr between $|\mathbf{B}| = 0.5$ and $1.0B_0$) as the charge transfer implied by the electronegativity difference is damped by the increasing total hardness of the atoms.

Before proceeding to compare these predictions of changes in bond polarity with magnetic field strength to the results of current DFT calculations on the molecules themselves in these conditions, it should be noted that the value of $|\mathbf{B}|$ at which the change in bond polarity will occur will depend significantly on the model used for calculating ΔN . The Huheey model used here is one of the simplest models available [59, 60] and as such the qualitative rather than quantitative nature of the prediction will form the focus of the present discussion. The qualitative prediction of a reversal in bond polarity resulting from an external magnetic field is remarkable and, to the best of our knowledge, not reported elsewhere in the literature; it is obvious to see how chemistry under these conditions may differ significantly from the zero-field case.

The energies, dipole moments and Mulliken populations of the HF, HCl and HBr molecules were calculated at the current DFT level with the cTPSS exchange-correlation functional in the presence of external magnetic fields of $|\mathbf{B}| = 0.0 - 0.8B_0$ for HF and $0.0 - 0.5B_0$ for HCl and HBr, applied parallel and perpendicular to the internuclear axis. Whilst their equilibrium geometries can be expected to change with magnetic field strength, [46, 96] and indeed this will be examined later in the present discussion, initially the analysis will consider molecules fixed at their zero-field equilibrium geometries. Maintaining a fixed geometry better allows the results to be understood in the conceptual DFT framework, corresponding to fixing the external potential v and extending the conceptual DFT response tree to include derivatives with respect to magnetic field \mathbf{B} in a similar way to that presented in Ref. [27] for the electric field \mathcal{E} , in which the conventional electric-field related response functions such as dipole moment, polarisability and first hyperpolarisability became part of an extended response function tree containing new chemical descriptors. For example, the electric dipole moment μ_e and magnetic dipole moment μ_m can be defined, respectively, as

$$\mu_e = \left(\frac{\partial E}{\partial \mathcal{E}} \right)_v \quad \mu_m = \left(\frac{\partial E}{\partial \mathbf{B}} \right)_v. \quad (28)$$

Maintaining a fixed geometry and therefore external potential allows an extended response function tree to be constructed, with derivatives with respect to the magnetic field yielding the additional terms

$$\begin{aligned} \left(\frac{\partial \mu}{\partial \mathbf{B}} \right)_v &= \left(\frac{\partial \mu_m}{\partial N} \right)_v = \left(\frac{\partial^2 E}{\partial \mathbf{B} \partial N} \right)_v \\ \left(\frac{\partial \eta}{\partial \mathbf{B}} \right)_v &= \left(\frac{\partial^2 \mu_m}{\partial N^2} \right)_v = \left(\frac{\partial^3 E}{\partial \mathbf{B} \partial N^2} \right)_v. \end{aligned} \quad (29)$$

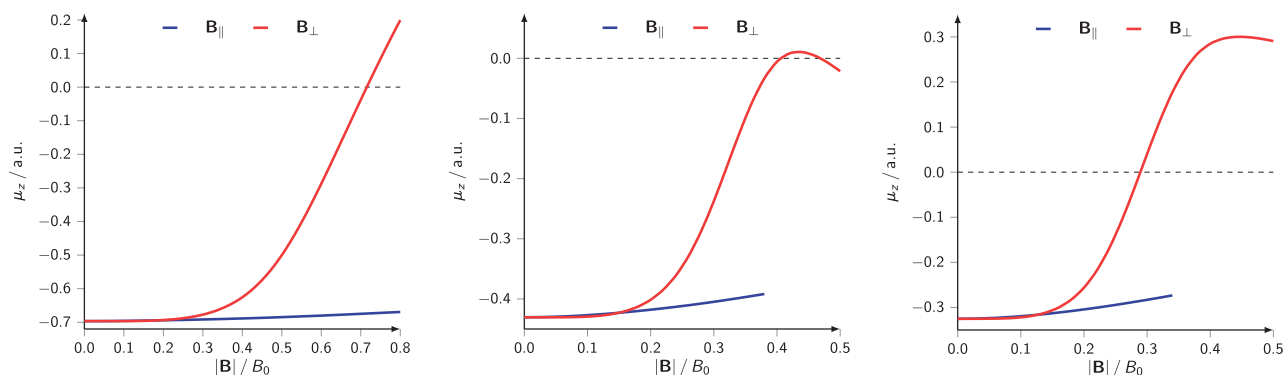


Figure 3. Electric dipole moment along the internuclear axis of HF (left), HCl (centre) and HBr (right) in atomic units as a function of external magnetic field strength $|\mathbf{B}| / B_0$ applied parallel and perpendicular to the bond.

In Figure 3, the electric dipole moment along the bond is shown for HF, HCl and HBr at their zero-field geometries as a function of magnetic field strength applied both parallel and perpendicular to the internuclear axis. As described above, the range $|\mathbf{B}| = 0.0 - 0.8B_0$ is considered for HF whilst for HCl and HBr this range is truncated to $|\mathbf{B}| = 0.0 - 0.5B_0$. In the latter two cases, the dipole moments in a parallel field cannot be computed at field strengths above $0.38B_0$ and $0.34B_0$, respectively, since a symmetry breaking occurs and a solution with a different electronic configuration results. The H – X bond is aligned along the z -axis with $R_z(H) < R_z(X)$ in all cases and the zero-field dipole moment has a negative sign (negative to positive convention).

At zero-field the electric dipole moments for HF, HCl and HBr are computed (in Debye) to be -1.771D , -1.094D and -0.827D , respectively; these are in reasonable agreement with the experimentally determined values of 1.826D , 1.109D and 0.827D , respectively, [97] and follows the trend expected from the decreasing electronegativity of the series $\text{F} \rightarrow \text{Cl} \rightarrow \text{Br}$.

For magnetic fields applied both parallel and perpendicular to the internuclear axis, it is observed that only the component of the electric dipole along to the internuclear axis has a non-zero value. This may be understood by analysing the symmetry of the system in a magnetic field: at zero field, the hydrogen halides belong to the $C_{\infty v}$ point group; in the presence of an external field, the symmetry becomes that of the system and field together.

In the first instance, only the unitary symmetry of the system and field shall be considered as it is the most commonly encountered type of symmetry [46, 98, 99]. The unitary symmetry group of a uniform magnetic field in the absence of any particles is $C_{\infty h}$. Thus, when the magnetic field is applied parallel to the internuclear axis, the unitary symmetry group of the system and field together becomes C_{∞} which contains only a C_{∞} proper rotation

axis along the H – X bond. By contrast, if the magnetic field is applied perpendicular to the internuclear axis, the system plus field unitary symmetry group then becomes C_s , with only a σ_h mirror plane perpendicular to the field.

It is clear from these arguments that, when a magnetic field is applied parallel to the H – X axis, only the electric dipole moment component along this direction may exist as this is the only component that remains invariant under the symmetry operations of the unitary symmetry group C_{∞} . Similarly, in the case of the perpendicular magnetic field, the two dipole moment components orthogonal to the field, one along the H – X axis, and one in the direction perpendicular to both the H – X axis and the applied field, are both permitted to be non-zero by the unitary symmetry group C_s . However, as revealed by the calculation results discussed so far, in both parallel- and perpendicular-magnetic-field cases, non-zero electric dipole moments are only ever observed along the H – X axis while any components perpendicular to this direction identically vanish.

To account for the unexpected vanishing of the dipole moment component orthogonal to both the H – X axis and the magnetic field in the perpendicular-field case, it is necessary to go beyond unitary symmetry. In fact, it turns out that the time-reversal operator $\hat{\theta}$ – an antiunitary operator under the action of which the direction of \mathbf{B} is inverted – must also be considered. The product of $\hat{\theta}$ and other unitary operators \hat{u} that act to reverse the direction of \mathbf{B} form a set of antiunitary operations under which \mathbf{B} is invariant. If the molecular symmetry group contains some of these unitary operators \hat{u} , then the full symmetry group of the molecule in the field also contains the corresponding antiunitary $\hat{\theta}\hat{u}$ products. In such a case, the full magnetic symmetry group is no longer unitary. These symmetry arguments are presented more formally and completely in the [Appendix](#).

In the case of the H – X molecule with a magnetic field applied perpendicular to its principal axis, considering only unitary symmetry transformations leads to the classification of this system as belonging to the unitary symmetry group C_s as described above. However, the molecular symmetry group $C_{\infty v}$ also contains the unitary C_2^\perp and σ_v operations which reverse the direction of \mathbf{B} . They can thus be combined with the antiunitary time-reversal operator $\hat{\theta}$ to yield the antiunitary operations $\hat{\theta}C_2^\perp$ and $\hat{\theta}\sigma_v$ that leave both \mathbf{B} and the nuclear framework unchanged. The full magnetic symmetry group of the system is therefore given by $\mathcal{M} = C_s + \hat{\theta}\{C_2^\perp, \sigma_v\}$ where the ‘+’ denotes a disjoint union. This symmetry group \mathcal{M} is isomorphic to C_{2v} with C_s being a normal subgroup of index two; by convention this may be labelled as $C_{2v}(C_s)$ [100, 101]. In this symmetry group, the electric dipole moment component perpendicular to both \mathbf{B} and the H – X bond is not invariant under $\hat{\theta}C_2^\perp$ and $\hat{\theta}\sigma_v$ and therefore must always vanish, as is indeed the case in the present calculations.

Returning to Figure 3, it can be seen in all three cases that the behaviour of the dipole moment with respect to magnetic field strength is significantly different where the field is applied perpendicular to the internuclear axis compared to where it is applied parallel to this axis. In a parallel magnetic field, there are only relatively minor changes to the electric dipole moment; in the case of HF, there is only a change of +0.027 a.u. as the magnetic field is increased from $|\mathbf{B}| = 0.0 - 0.8B_0$. By contrast, there is a much more significant change to the electric dipole moment in the presence of a perpendicular magnetic field, with it becoming less negative much more rapidly with increasing magnetic field strength than when applied parallel to the bond and eventually changing sign, revealing a reversal of bond polarity. In the case of HF, the dipole moment changes from -0.697 a.u.

at zero field to +0.200 a.u. at $|\mathbf{B}| = 0.8B_0$ perpendicular to the bond, with the change in sign occurring at $|\mathbf{B}| = 0.72B_0$; in all cases with no change of electronic configuration.

This change in bond polarity can be further investigated by looking at the change in Mulliken charge on the hydrogen atom with increasing field strength, shown for HF, HCl and HBr in Figure 4 along with the charge transfer $-\Delta N$ predicted by the Huheey model with Equation (11).

It can be seen in Figure 4 that the Mulliken charge on the hydrogen atom becomes somewhat smaller with increasing magnetic field strength applied parallel to the internuclear axis, but decreases much more rapidly with increasing field strength perpendicular to the internuclear axis, in all three cases becoming negative at a similar magnetic field strength to that at which the electric dipole moment changes sign. In the case of HF, the Mulliken charge on the hydrogen atom goes from +0.306 at zero field to +0.180 in a magnetic field of $|\mathbf{B}| = 0.8B_0$ parallel to the bond but -0.200 when the field is oriented perpendicular to the bond, confirming the change in bond polarity observed with the reversal of the electric dipole moment.

For the HF molecule, the changes in electric dipole moment and Mulliken charge in strong magnetic fields parallel and perpendicular to the internuclear axis were also calculated using Hartree-Fock and the range-separated exchange hybrid form of cTPSS (cTPSSrsh) [102]. This was to investigate the possible effect the over-delocalisation of charge density associated with DFT exchange-correlation functionals such as TPSS on the propensity for a transfer of charge to occur between the hydrogen and fluorine atoms in a strong magnetic field. The over-delocalisation of charge density could result in the change in the direction of charge transfer occurring

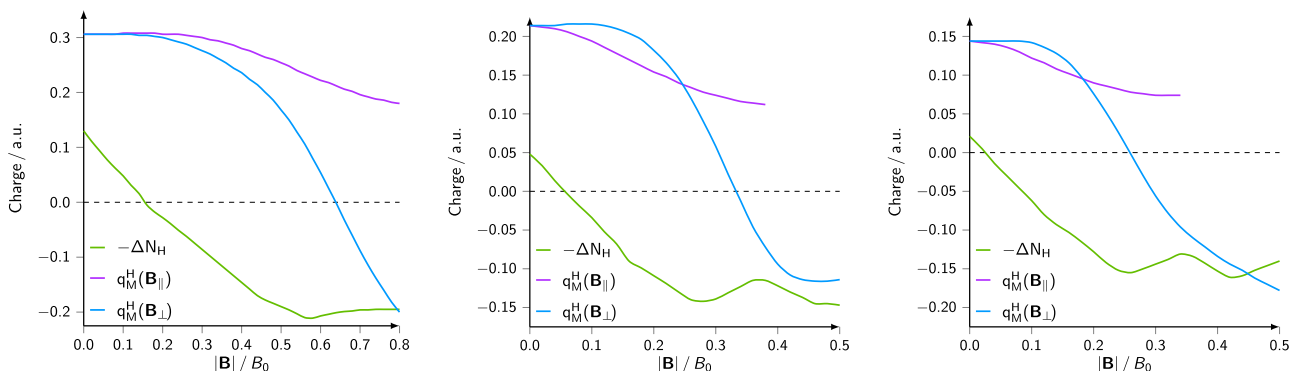


Figure 4. Mulliken charges on the hydrogen atom q_M^H in HF (left), HCl (centre) and HBr (right) in as a function of external magnetic field strength $|\mathbf{B}| / B_0$ applied parallel and perpendicular to the bond, with the charge transfer to the hydrogen atom $-\Delta N_H$ predicted by the Huheey model given for comparison.

at an erroneously low magnetic field strength. In contrast, the charge-density is over-localised with Hartree-Fock which could result in the change in direction of charge transfer occurring at an erroneously high magnetic field strength. The cTPSSrsh exchange functional combines TPSS exchange at short-range with Hartree-Fock exchange at long-range, which should lead to an improvement on the delocalisation error of cTPSS by ensuring the exchange-potential has the correct asymptotic behaviour. For the HF molecule, only small differences in the change of electric dipole moment and Mulliken charge with magnetic field were observed between HF, cTPSS and cTPSSrsh – this is discussed further in the Supporting Information. This indicates that, for the small molecules considered in this work, the effects of charge over-localisation with Hartree-Fock and over-delocalisation with cTPSS are not significant and do not need explicit consideration here.

These changes in bond polarity in a strong magnetic field are qualitatively in line with what would be predicted from the atomic electronegativity and hardness values at these field strengths. It can be seen however in Figure 4 that the field strength at which the change in bond polarity would be expected to occur according to the Huheey model of Equation (11) is consistently much lower than that at which it is observed to actually occur in the molecular calculations. As described earlier, this is to be expected in view of the approximate nature of the Huheey equation, in particular its neglect of the external potential and the parabolic approximation of the $E(N)$ curve [17]. In the case of the hydrogen atom, with a high ionisation energy and low electron affinity, this approach is less appropriate than, for example, the exponential model later introduced by Parr and Bartolotti [103]. Furthermore, we note that the prediction of bond polarity from the atomic reactivity descriptors does not distinguish between orientations of the bond with respect to

the magnetic field since it is based on the global atomic descriptors χ and η . Whilst this is another limitation of this approach, intuitively one might expect the prediction to be most meaningful for the orientation of field with respect to the bond in which the effect on the bond polarity is greatest – in this case, perpendicular.

The change in bond polarity occurring in a strong magnetic field applied perpendicular to the internuclear axis but not applied parallel can be seen clearly by plotting the charge density of the molecule under these two magnetic fields relative to the charge density of the molecule at zero field. This is shown for HF in Figure 5 in a magnetic field of $|\mathbf{B}| = 0.8B_0$ parallel and perpendicular to the bond.

Figure 5 reveals that, in a magnetic field parallel to the H – F bond, there is no transfer of charge density along this axis. Instead, there is a general accumulation of charge density around the nuclei relative to zero field, with a general depletion of charge density beyond this region – most likely reflecting the contraction of charge density that occurs in strong magnetic fields [104–106]. By contrast, in a perpendicular field there is a clear and significant depletion of charge density around the fluorine atom and accumulation of charge density around the hydrogen atom, relative to zero-field, providing further evidence of the shift in charge distribution associated with the reversal in bond polarity arising in a strong perpendicular magnetic field.

This result is significant; not only does an inversion of bond polarity occur in a diatomic molecule under the influence of an applied magnetic field, but these results observed from molecular current DFT calculations confirm the qualitative predictions made using ideas from conceptual DFT and atomic reactivity indicators computed under these conditions in the previous study [24], thus confirming the utility of this approach.

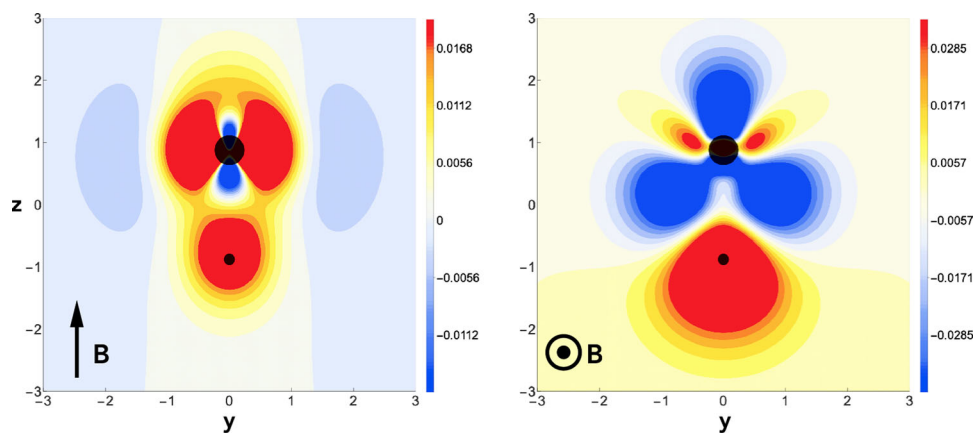


Figure 5. Difference in charge density of HF in a magnetic field of $|\mathbf{B}| = 0.8B_0$ applied parallel (left) and perpendicular (right) to the internuclear axis, relative to that at zero field.

The picture for HCl and HBr in strong magnetic fields is similar although not identical to that for HF. Figure 3 shows that a magnetic field applied parallel to the internuclear axis of HCl and HBr has a relatively modest effect on the electric dipole moment, only increasing by +0.039 a.u. in HCl between zero-field and $|\mathbf{B}| = 0.38B_0$ and +0.052 a.u. in HBr between zero-field and $|\mathbf{B}| = 0.34B_0$; in both cases, this is the maximum field strength at which the zero-field electronic configuration can be obtained. As with HF, there is a much more significant change in the electric dipole moment in a perpendicular magnetic field; a change in sign of the electric dipole occurs at $|\mathbf{B}| = 0.42B_0$ in HCl and $|\mathbf{B}| = 0.30B_0$ in HBr, the field strength becoming progressively lower for molecules with smaller zero-field dipole moments. Interestingly, the Mulliken charge of the hydrogen atom at the field strength where the sign of the dipole moment reverses in HCl is -0.108 and in HBr is -0.056 , implying that the reversal in bond polarity has already occurred at a slightly lower field strength than that at which the electric dipole moment changes sign.

Remarkably, even though no changes in electronic configuration occur, the dipole moment in HCl reaches a maximum value of around +0.01 a.u. at $|\mathbf{B}| = 0.44B_0$, before then decreasing as the field strength increases further, crossing zero again at $|\mathbf{B}| = 0.48B_0$ and becoming more negative with increasing field strength. A similar trend is present in HBr, with the dipole moment reaching a maximum value of +0.30 a.u. at $|\mathbf{B}| = 0.44B_0$ before beginning to decrease with increasing magnetic field strength; the difference from HCl is the maximum value the dipole moment reaches before the trend with increasing magnetic field strength reverses again.

It is interesting to compare the effects of an applied magnetic field on bond polarity with those that occur due to an applied electric field. It was previously shown by

Ramos *et al.*, approximating the electric field with various models, that a relatively small evolution in the dipole moment of HF occurs when the electric field is applied parallel to the internuclear axis up to a field strength of $5.2 \times 10^{10} \text{ Vm}^{-1}$, roughly equivalent to 0.1 a.u., however these electric fields are parallel to the direction of the electric dipole moment so a change in polarity would never be expected [56].

In the present work, we present complete calculations using the OEFF approach with an electric field applied parallel and perpendicular to the internuclear axis, with a field strength of $|\mathcal{E}| = 0.0 - 0.1$ a.u. for HF and $|\mathcal{E}| = 0.0 - 0.05$ a.u. for HCl and HBr; values in the range typically used in OEFF studies and within experimental reach. The evolution of the electric dipole moment with field strength for these three molecules at fixed geometry and zero magnetic field is presented in Figure 6.

A uniform electric field in the absence of any particles transforms according to the $C_{\infty v}$ point group and therefore, when applied parallel to the internuclear axis of the HX molecules, the overall unitary symmetry group of the system and external electric field combined remains $C_{\infty v}$. Unlike the cases of external magnetic fields, it is not necessary to go beyond unitary symmetry here because electric fields are not affected by the antiunitary action of time reversal. It follows that $C_{\infty v}$ is indeed the full symmetry group of the system and field, in which the electric dipole may only be non-zero along the principal axis. By orienting \mathcal{E} antiparallel to the zero-field electric dipole moment, it can be seen in Figure 6 that it becomes less negative with increasing field strength, changing sign at $|\mathcal{E}| = 0.082, 0.024$ and 0.012 a.u. for HF, HCl and HBr, respectively, and continuing to increase with increasing field strength in all cases.

With a uniform electric field applied perpendicular to the internuclear axis, the overall unitary symmetry group

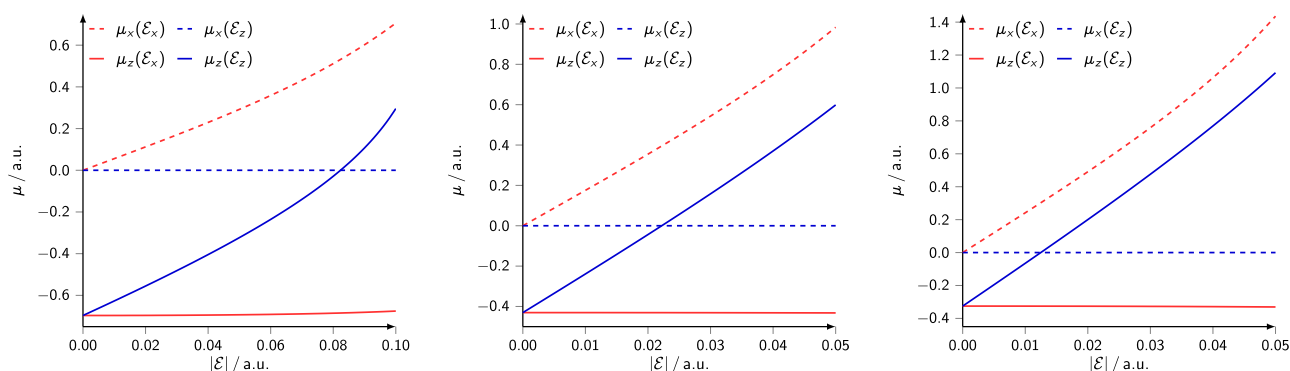


Figure 6. Components of the electric dipole moment parallel (μ_z) and perpendicular (μ_x) to the internuclear axis of HF (left), HCl (centre) and HBr (right) in atomic units as a function of external electric field strength $|\mathcal{E}|$ / a.u. applied parallel (\mathcal{E}_z) and perpendicular (\mathcal{E}_x) to the bond.

of the system and field together reduces to \mathcal{C}_s with only the σ_v plane containing both the electric field and the HX molecule remaining. A non-zero component of the electric dipole moment in the direction of the applied field, whilst perpendicular to the internuclear axis, is not symmetry forbidden and indeed it can be seen in Figure 6 that, with such an electric field applied, the change in electric dipole moment in this direction perpendicular to the bond is much more significant than that along the bond. For HF over the range of $|\mathcal{E}| = 0.0 - 0.1$ a.u. perpendicular to the H - F bond, the component of the dipole moment parallel to the bond increases by only +0.021 a.u. whilst the component perpendicular to the H - F bond and parallel to the applied field increases by +0.706 a.u. A similar picture is seen for HCl and HBr where, with an electric field of $|\mathcal{E}| = 0.0 - 0.05$ a.u. perpendicular to the bond, the component of the electric dipole parallel to the bond changes by -0.002 a.u. and -0.005 a.u. for HCl and HBr, respectively, whilst the components perpendicular to the bond and parallel to the applied field vector increase by +0.984 and +1.436 for HCl and HBr, respectively.

Considering the three molecules together, a common pattern emerges: in the presence of a strong magnetic field, relatively modest changes to dipole moment and charge distribution are seen when the field is applied parallel to the internuclear axis however much more significant changes are observed where the field is applied perpendicular to this axis. In all three cases, the electric dipole moment becomes less negative with increased perpendicular magnetic field strength, crossing zero at $|\mathbf{B}| = 0.72, 0.42$ and $0.30B_0$ for HF, HCl and HBr, respectively - indicative that the higher the zero field bond polarity, the greater the field strength required for its inversion. This pattern is also reflected in the behaviour of the Mulliken charges for the hydrogen atom in these three molecules with increasing field strength.

It would appear from a preliminary analysis of Figure 3 that HCl is something of an outlier, since the dipole moment only attains a small positive value, decreasing again with increasing field strength and becoming negative again. However, similar behaviour is exhibited in HBr - in which the dipole moment reaches a maximum positive value at some magnetic field strength, beyond which it begins to decrease again. A provisional study of HF at higher magnetic field strengths than those considered in the present discussion suggests similar behaviour is exhibited for this molecule, with the dipole moment reaching a maximum value at around $|\mathbf{B}| = 1.20B_0$ and decreasing beyond this point. However, these results are only provisional and should be treated with caution, since the quality of the basis set can deteriorate significantly at higher field strengths, necessitating a larger basis set with

higher angular momentum functions to adequately represent the increasingly distorted charge density [36, 102].

This is in contrast to the effect of an applied electric field, which applied (anti)parallel to the internuclear axis induces an inversion of the dipole moment at $|\mathcal{E}| = 0.082, 0.024$ and 0.012 a.u. for HF, HCl and HBr, respectively. However, as for the case of an applied magnetic field, the greater the zero-field dipole moment then the larger the applied field required for it to be reversed.

By analogy to the calculation of the zero-field response of the electronegativity to an applied magnetic field for atoms presented in Ref. [24], the response of the electric dipole moment to an applied magnetic field and applied electric field can be evaluated by finite difference at small values of the field. These are summarised for the components of the electric dipole which are not symmetry-forbidden in Table 2.

It can be seen in Table 2 that the zero-field response of the electric dipole to the magnetic field is very small - being slightly positive for the field parallel to the dipole and slightly negative for the field perpendicular to the dipole. Whilst perhaps surprising that the zero-field response is relatively small, it is concordant with observations of Figure 3, in which it can be seen that significant changes to the dipole moment do not occur near zero-field but begin to become discernible at much higher field strengths. In comparison, with an applied electric field the response of the component of the electric dipole moment parallel to the electric field vector is significant for all three molecules; the positive values and uniform increase from HF \rightarrow HCl \rightarrow HBr is as expected based on the increasing polarisability of the halogen atoms (3.76, 14.7 and 20.6 a.u. for F, Cl and Br, respectively, [97]) going down that group in the periodic table.

To complete the investigation of the hydrogen halides, we finally considered the effect of geometry relaxation with increasing magnetic field strength on the corresponding evolution of the electric dipole moment. Whilst maintaining a fixed geometry permits the definition of response functions at a fixed external potential such as those in Table 2, recent studies have shown that the equilibrium geometry of even simple diatomic molecules can

Table 2. Zero-field response of the symmetry-permitted components of the electric dipole moment of the hydrogen halides to the application of an electric or magnetic field aligned parallel and perpendicular to the zero-field dipole, evaluated by finite difference.

	$\left(\frac{\partial \mu_{e,z}}{\partial B_x}\right)_v$	$\left(\frac{\partial \mu_{e,z}}{\partial B_z}\right)_v$	$\left(\frac{\partial \mu_{e,x}}{\partial \mathcal{E}_x}\right)_v$	$\left(\frac{\partial \mu_{e,z}}{\partial \mathcal{E}_x}\right)_v$	$\left(\frac{\partial \mu_{e,z}}{\partial \mathcal{E}_z}\right)_v$
HF	0.00002	-0.00012	5.56872	0.00000	6.90474
HCl	0.00009	-0.00075	17.46719	-0.00001	19.02715
HBr	0.00015	-0.00158	24.03078	-0.00004	25.85462

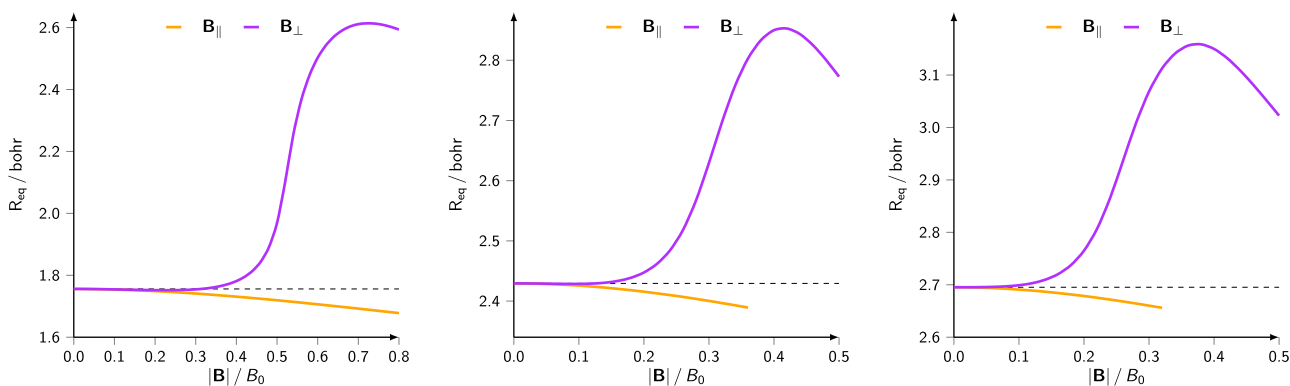


Figure 7. Equilibrium bond length of HF (left), HCl (centre) and HBr (right) as a function of external magnetic field strength $|\mathbf{B}| / B_0$ applied parallel and perpendicular to the bond.

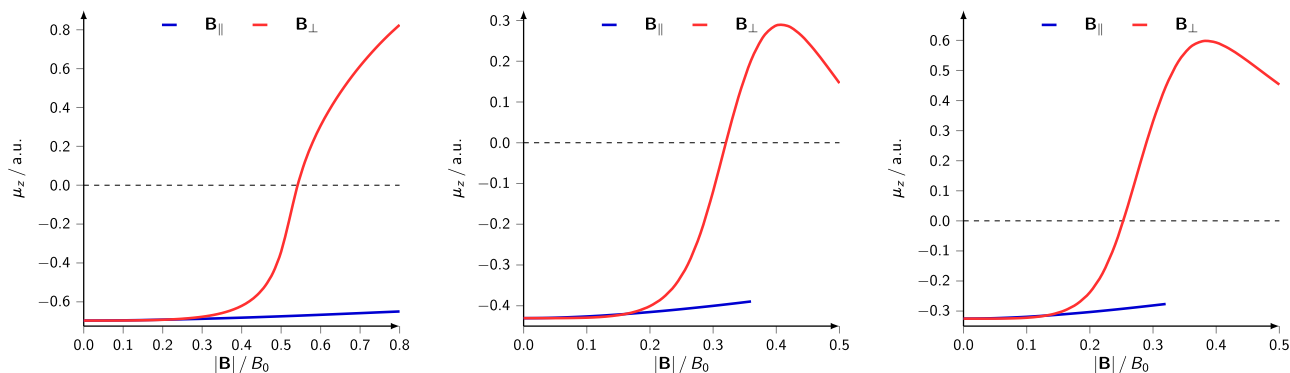


Figure 8. Electric dipole moment along the internuclear axis of HF (left), HCl (centre) and HBr (right) in atomic units at their equilibrium bond lengths as a function of external magnetic field strength $|\mathbf{B}| / B_0$ applied parallel and perpendicular to the bond.

change significantly in the presence of strong magnetic field, in a way that depends on the orientation of the field relative to the bond [40, 46, 96]. Using the analytical gradient implementation presented in Ref. [46], the geometries of the hydrogen halides were optimised in the presence of magnetic fields applied parallel and perpendicular to the bond over the range of field strengths considered for the fixed-bond lengths. The change in the equilibrium bond length as a function of field strength is shown in Figure 7.

In all cases, Figure 7 shows that the equilibrium bond length shows a slight decrease with increasing magnetic field strength parallel to the bond, but a much more significant increase with magnetic field strength perpendicular to the bond, with maxima in the equilibrium bond length with respect to field strength observed for all three molecules. Clearly these significant changes to the equilibrium bond length would be expected to affect the dipole moment, which in its most basic definition is simply the difference between two charges multiplied by their separation. The electric dipole moment as a function of the magnetic field strength is presented in an analogous manner to that for fixed bond lengths in Figure 8.

It can be seen in Figure 8 that, whilst the fundamental trends discussed for the fixed bond length calculations such as the relative field strengths at which the dipole moment changes sign for the three molecules remain unchanged, the picture is significantly affected by the relaxation of the geometry. In particular, for the magnetic field perpendicular to the internuclear axis, the field strength at which the dipole moment changes sign is reduced to $|\mathbf{B}| = 0.54, 0.32$ and $0.26B_0$ for HF, HCl and HBr, respectively. Furthermore, the maximum change in the dipole moment over the range of field strengths is larger: increasing from $0.896 \text{ a.u.} \rightarrow 1.522 \text{ a.u.}$ for HF, $0.441 \text{ a.u.} \rightarrow 0.718 \text{ a.u.}$ for HCl and $0.625 \text{ a.u.} \rightarrow 0.923 \text{ a.u.}$ for HBr; observations that would be expected given the associated increase in equilibrium geometry.

3.2. H_2O and NH_3

Finally, we extend the study to the evolution of the dipole moment of H_2O and NH_3 in a magnetic field.

3.2.1. H_2O

In the case of H_2O , when the magnetic field is applied along the C_2 axis of the molecule (which will henceforth

be referred to as the ‘parallel-field’ case), the unitary symmetry group of the combined molecule and field is C_2 , but the full magnetic symmetry group taking into account the antiunitary action of time reversal is $C_{2v}(C_2)$. By contrast, when the magnetic field is applied perpendicular to the plane of the molecule (which will henceforth be referred to as the ‘perpendicular-field’ case), the unitary symmetry group is C_s and the full magnetic symmetry group is $C_{2v}(C_s)$.

In the calculations where the H_2O molecule is placed in the yz -plane with the C_2 axis along z , a consideration of only unitary symmetry shows that a variation of the dipole moment along the z -axis is expected in both cases, but also along the x -axis in the perpendicular case. However, when time reversal is taken into account, in analogy with the hydrogen halides, the x -component in the case of a perpendicular field must also vanish. The evolution of the z -component for the parallel- and perpendicular-field cases is now more similar than in the case of the hydrogen halides, shown on the left of Figure 9.

It can be seen in Figure 9 that the dipole moment becomes less negative with increasing magnetic field strength in both cases, changing sign with a perpendicular field of around $|\mathbf{B}| = 0.80B_0$. As for HCl and HBr, a symmetry breaking at increased field strength prevents the dipole moment from being calculated across the full range of field strengths with a consistent state with a parallel field.

The case with an applied electric field can be seen on the right of Figure 9. A similarity with the parallel-magnetic field case can be noted; the corresponding full symmetry group C_{2v} giving rise to a single dipole moment component along the z -axis, which is seen to change sign upon increasing field strength (oriented along the $+z$ -direction). The case of the perpendicular electric field with resulting symmetry group C_s permits non-vanishing

dipole moment components along the z - and x -axes, as opposed to a single component in the magnetic field case. This is observed in Figure 9, where the largest changes in dipole moment with a perpendicular electric field occur along the x -axis.

The significant effect on the polarity of H_2O and therefore the charge distribution by applied electric and magnetic fields suggests that permanent dipole-permanent dipole interactions will be significantly affected by these external fields. Future work considering the change in charge distributions of water dimers and possibly larger systems, informed by the work of Ref. [48], should help provide additional insight to the unresolved question of the overall effect of magnetic fields on hydrogen bonding.

3.2.2. NH_3

Intuitively, similar results are expected for NH_3 though of course the symmetry of the system, which plays an important role in all our discussions, is not the same. For a magnetic field parallel to the molecular C_3 axis oriented along the z -direction (‘parallel-field’ case), the unitary symmetry group is C_3 and the full magnetic symmetry group taking into account time reversal is $C_{3v}(C_3)$. Under both groups, μ_z turns out to be the only allowed dipole moment component. It shows the expected decrease (in absolute value) upon increasing field strength though an inversion of polarity is not observed at this geometry. This inversion on the other hand is observed in the parallel-electric-field case (the symmetry group of the system being C_{3v} is identical to that of the isolated molecule and unaltered by the field). This can be seen in Figure 10.

By contrast, when a magnetic field is applied perpendicular to the molecular C_3 axis along the z -direction and also to the σ_v^{yz} plane (‘perpendicular-field’ case), both the unitary symmetry group and the full magnetic symmetry group are C_s , allowing two non-vanishing electric

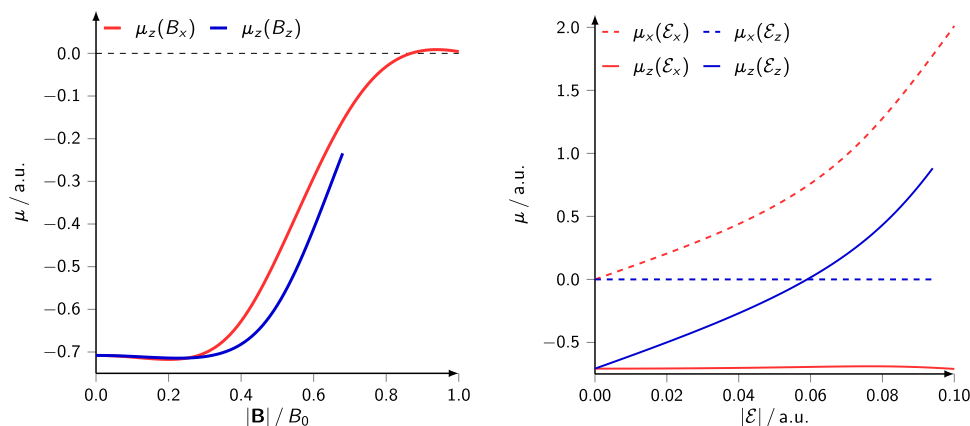


Figure 9. Components of the electric dipole moment parallel to the C_2 axis of H_2O (μ_z) and perpendicular to the plane of H_2O (μ_x) in atomic units as a function of external magnetic field strength $|\mathbf{B}|/B_0$ (left) and electric field strength $|\mathcal{E}|/a.u.$ (right).

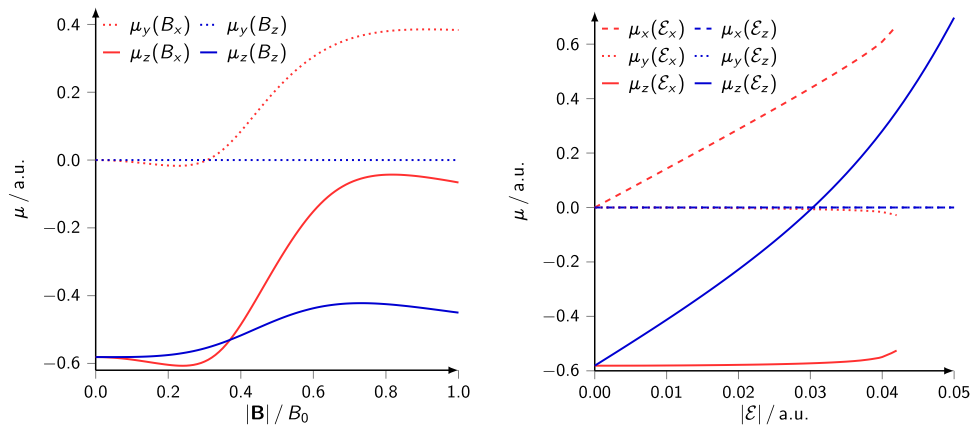


Figure 10. Components of the electric dipole moment parallel to the C_3 axis of NH_3 (μ_z) and perpendicular to this axis (μ_x, μ_y) in atomic units as a function of external magnetic field strength $|\mathbf{B}|/B_0$ (left) and electric field strength $|\mathcal{E}|/a.u.$ (right).

dipole components (μ_z and μ_y) which now, as opposed to the H_2O case, indeed survive – as can be seen in Figure 10. The z -component shows, not unexpectedly, an almost inverted polarity at the highest fields, whilst the y -component, zero in the field-free case, shows a similar increase. In the case of a perpendicular electric field applied, the symmetry of the system is C_1 and as such the electric dipole moment can be non-zero in all three Cartesian directions. This can be seen in Figure 10 where, with a perpendicular electric field applied, there is a large change in μ_x and small but non-zero changes to μ_y and μ_z .

Overall, the results for NH_3 bear large similarity with the H_2O case, although the symmetry of these molecules in the presence of magnetic fields must be carefully considered in the interpretation of these observations.

4. Conclusions

In this work, the influence of strong magnetic fields on the charge distribution – as manifested by the electric dipole moment, atomic partial charges and charge densities themselves – on the hydrogen halides is considered in two different ways. The first of these is with a conceptual DFT model, making use of the atomic electronegativity and hardness evaluated in Ref. [24] across a range of magnetic field strengths for atoms H-Kr, with which the charge transfer within a bond can be predicted in the presence of a strong magnetic field. The second approach is through current DFT calculations on the molecules themselves, with a strong magnetic field applied parallel and perpendicular to the internuclear axis and with the electric dipole moment and Mulliken charges evaluated from the converged solutions. The inversion of polarity predicted by the conceptual DFT model, and the trend expected for the three halogen atoms, is observed in the current DFT calculations – with an inversion in polarity

of HF, HCl and HBr with a strong magnetic field applied perpendicular to the internuclear axis, at decreasing magnetic field strength in the series $\text{HF} \rightarrow \text{HCl} \rightarrow \text{HBr}$. The central role of symmetry in determining the components of the dipole moment which are non-zero is seen in the comparison between the results from an applied electric and magnetic field; in the latter case, consideration of time reversal symmetry is essential to understanding which components of the dipole moment vanish and which do not. Analysis of the Mulliken populations and of the change in charge density itself confirms that the reversal of the dipole moment in these systems is in line with the shift in charge distribution in strong magnetic fields. The present work highlights the need to consider the full magnetic symmetry group. This is expected to be essential, for example, in utilising symmetry to understand electronic spectra and selection rules for allowed transitions in magnetic fields.

At a fixed geometry, the response of the dipole moment to an external magnetic field $(\partial \mu_e / \partial \mathbf{B})_v$ can be included in an extended conceptual DFT response function tree and is seen to be equal to the second derivative of the energy with respect to electric and magnetic field. Permitting the geometry to relax, it is seen that the equilibrium bond length of the hydrogen halides decreases slightly with increasing magnetic field strength parallel to the bond whereas it increases significantly in a perpendicular field.

The results for H_2O and NH_3 are, in general, consistent with the results seen for the hydrogen halides – with changes in the dipole moment and inversions of its direction in the presence of external electric and magnetic fields of certain orientations relative to the principal axes of these molecules. These observations may be useful for guiding further studies on clusters of these molecules, to provide new insight into the unresolved question of the influence of magnetic fields on hydrogen bonding. The

results for NH₃ show strong similarities with those of H₂O however, though a full consideration of the symmetry properties of these systems in the presence of magnetic fields, the perhaps unexpected differences between these can be understood.

Acknowledgements

The authors want to dedicate this paper to Professor B.M. Deb on the occasion of his 80th birthday. Professor Deb has been an outstanding quantum chemist for decades and has played a pioneering role in the study of behaviour of systems in electromagnetic fields. For one (PG) of us it has been a great pleasure and privilege to meet him several times in India, discussing science and listening to his vast knowledge about the culture of his marvellous country.

Disclosure statement

No potential conflict of interest was reported by the authors.

Funding

We acknowledge financial support from the European Research Council under H2020/ERC Consolidator Grant top DFT [grant number 772259]. We are grateful for access to the University of Nottingham Augusta HPC service. FDP and PG are thankful to the Vrije Universiteit Brussel for a long-term grant of a Strategic Research Program.

ORCID

Tom J. P. Irons  <http://orcid.org/0000-0001-5527-6002>
 Bang C. Huynh  <http://orcid.org/0000-0002-5226-4054>
 Andrew M. Teale  <http://orcid.org/0000-0001-9617-1143>
 Frank De Proft  <http://orcid.org/0000-0003-4900-7513>
 Paul Geerlings  <http://orcid.org/0000-0003-1897-7285>

References

- [1] S. Ciampi, N. Darwish, H.M. Aitken, I. Díez-Pérez and M.L. Coote, *Chem. Soc. Rev.* **47** (14), 5146–5164 (2018). doi:10.1039/C8CS00352A
- [2] S. Shaik, R. Ramanan, D. Danovich and D. Mandal, *Chem. Soc. Rev.* **47** (14), 5125–5145 (2018). doi:10.1039/C8CS00354H
- [3] M.K. Beyer and H. Clausen-Schaumann, *Chem. Rev.* **105** (8), 2921–2948 (2005). doi:10.1021/cr030697h
- [4] C.R. Hickenboth, J.S. Moore, S.R. White, N.R. Sottos, J. Baudry and S.R. Wilson, *Nature* **446** (7134), 423–427 (2007). doi:10.1038/nature05681
- [5] W. Grochala, R. Hoffmann, J. Feng and N.W. Ashcroft, *Angew. Chem. – Int. Ed.* **46** (20), 3620–3642 (2007). doi:10.1002/(ISSN)1521-3773
- [6] M. Rahm, R. Cammi, N.W. Ashcroft and R. Hoffmann, *J. Am. Chem. Soc.* **141** (26), 10253–10271 (2019). doi:10.1021/jacs.9b02634
- [7] S. Shaik and T. Stuyver, editors, *Effects of Electric Fields on Structure and Reactivity* (Royal Society of Chemistry, Cambridge, 2021).
- [8] T. Stauch and A. Dreuw, *Chem. Rev.* **116** (22), 14137–14180 (2016). doi:10.1021/acs.chemrev.6b00458
- [9] D. Margetic, *High Pressure Organic Synthesis* (De Gruyter, Berlin, 2019).
- [10] M. Xu, Y. Li and Y. Ma, *Chem. Sci.* **13** (2), 329–344 (2022). doi:10.1039/D1SC04239D
- [11] J.R.P. Angel and J.D. Landstreet, *Astrophys. J.* **191**, 457 (1974). doi:10.1086/152984
- [12] J.R.P. Angel, *Astrophys. J.* **216**, 1 (1977). doi:10.1086/155436
- [13] D. Lai, *Rev. Modern Phys.* **73** (3), 629–662 (2001). doi:10.1103/RevModPhys.73.629
- [14] O.A. Al-Hujaj and P. Schmelcher, *Phys. Rev. A* **70** (3), 033411 (2004). doi:10.1103/PhysRevA.70.033411
- [15] M.V. Ivanov and P. Schmelcher, *Phys. Rev. A* **60** (5), 3558–3568 (1999). doi:10.1103/PhysRevA.60.3558
- [16] O.A. Al-Hujaj and P. Schmelcher, *Phys. Rev. A* **70** (2), 023411 (2004). doi:10.1103/PhysRevA.70.023411
- [17] R.G. Parr and W. Yang, *Density Functional Theory of Atoms and Molecules* (Oxford University Press, Oxford, United Kingdom, (1989).
- [18] R.G. Parr and W. Yang, *Annu. Rev. Phys. Chem.* **46** (1), 701–728 (1995). doi:10.1146/physchem.1995.46.issue-1
- [19] H. Chermette, *J. Comput. Chem.* **20** (1), 129–154 (1999). doi:10.1002/(ISSN)1096-987X
- [20] P. Geerlings, F. De Proft and W. Langenaeker, *Chem. Rev.* **103** (5), 1793–1874 (2003). doi:10.1021/cr990029p
- [21] P.W. Ayers, J.S.M. Anderson and L.J. Bartolotti, *Int. J. Quantum Chem.* **101** (5), 520–534 (2004). doi:10.1002/(ISSN)1097-461X
- [22] P. Geerlings, E. Chamorro, P.K. Chattaraj, F. De Proft, J.L. Gázquez, S. Liu, C. Morell, A. Toro-Labbé, A. Vela and P. Ayers, *Theor. Chem. Acc.* **139** (2), 36 (2020). doi:10.1007/s00214-020-2546-7.
- [23] S. Liu, editor, *Conceptual Density Functional Theory* (Wiley-VCH, Weinheim, Germany, 2022).
- [24] R. Francotte, T.J.P. Irons, A.M. Teale, F. De Proft and P. Geerlings, *Chem. Sci.* **13** (18), 5311–5324 (2022). doi:10.1039/D1SC07263C
- [25] M. Franco-Pérez, P.W. Ayers, J.L. Gázquez and A. Vela, *J. Chem. Phys.* **143** (24), 244117 (2015). doi:10.1063/1.4938422
- [26] J.L. Gázquez, M. Franco-Pérez, P.W. Ayers and A. Vela, *Int. J. Quantum Chem.* **119** (2), e25797 (2018). doi:10.1002/qua.v119.2
- [27] T. Clarys, T. Stuyver, F. De Proft and P. Geerlings, *Phys. Chem. Chem. Phys.* **23** (2), 990–1005 (2021). doi:10.1039/D0CP05277A
- [28] T. Bettens, M. Alonso, P. Geerlings and F. De Proft, *Phys. Chem. Chem. Phys.* **21** (14), 7378–7388 (2019). doi:10.1039/C8CP07349J
- [29] T. Bettens, M. Alonso, P. Geerlings and F. De Proft, *Chem. Sci.* **11** (5), 1431–1439 (2020). doi:10.1039/C9SC04507D
- [30] A. Borgoo, D.J. Tozer, P. Geerlings and F. De Proft, *Phys. Chem. Chem. Phys.* **11** (16), 2862 (2009). doi:10.1039/b820114e
- [31] P. Geerlings, D.J. Tozer and F. De Proft, in *Chemical Reactivity in Confined Systems*, edited by P. K. Chattaraj and D. Chakraborty (Wiley, Hoboken, NJ, 2021), Chap. 3, pp. 49–67.

- [32] J. Eeckhoudt, T. Bettens, P. Geerlings, R. Cammi, B. Chen, M. Alonso and F. De Proft, *Chem. Sci.* **13** (32), 9329–9350 (2022). doi:10.1039/D2SC00641C
- [33] T. Detmer, P. Schmelcher, F.K. Diakonov and L.S. Cederbaum, *Phys. Rev. A* **56** (3), 1825–1838 (1997). doi:10.1103/PhysRevA.56.1825
- [34] T. Detmer, P. Schmelcher and L.S. Cederbaum, *Phys. Rev. A* **57** (3), 1767–1777 (1998). doi:10.1103/PhysRevA.57.1767
- [35] P. Schmelcher and L.S. Cederbaum, *Int. J. Quantum Chem.* **64** (5), 501–511 (1997). doi:10.1002/(SICI)1097-461X(1997)64:5<j.1.0.CO;2-7
- [36] S. Lehtola, M. Dimitrova and D. Sundholm, *Mol. Phys.* **118** (2), e1597989 (2019). doi:10.1080/00268976.2019.1597989
- [37] LONDON, A quantum chemistry program for plane-wave/GTO hybrid basis sets and finite magnetic field calculations londonprogram.org.
- [38] E.I. Tellgren, A. Soncini and T. Helgaker, *J. Chem. Phys.* **129** (15), 154114 (2008). doi:10.1063/1.2996525
- [39] F. London, *J. Phys. Radium* **8** (10), 397–409 (1937). doi:10.1051/jphysrad:01937008010039700
- [40] K.K. Lange, E.I. Tellgren, M.R. Hoffmann and T. Helgaker, *Science* **337** (6092), 327–331 (2012). doi:10.1126/science.1219703
- [41] C. Holzer, A. Pausch and W. Klopper, *Front. Chem.* **9**, 746162 (2021). doi:10.3389/fchem.2021.746162
- [42] F. Hampe, N. Gross and S. Stopkowicz, *Phys. Chem. Chem. Phys.* **22** (41), 23522–23529 (2020). doi:10.1039/D0CP04169F
- [43] T. Shiozaki, *WIREs Comput. Mol. Sci.* **8** (1), e1331 (2017). doi:10.1002/wcms.2018.8.issue-1
- [44] QUEST, A rapid development platform for quantum electronic structure techniques quest.codes, 2020.
- [45] M. Wibowo, T.J.P. Irons and A.M. Teale, *J. Chem. Theory Comput.* **17** (4), 2137–2165 (2021). doi:10.1021/acs.jctc.0c01269
- [46] T.J.P. Irons, G. David and A.M. Teale, *J. Chem. Theory Comput.* **17** (4), 2166–2185 (2021). doi:10.1021/acs.jctc.0c01297
- [47] G. David, T.J.P. Irons, A.E.A. Fouda, J.W. Furness and A.M. Teale, *J. Chem. Theory Comput.* **17** (9), 5492–5508 (2021). doi:10.1021/acs.jctc.1c00236
- [48] B.T. Speake, T.J.P. Irons, M. Wibowo, A.G. Johnson, G. David and A.M. Teale, *J. Chem. Theory Comput.* (2022). doi:10.1021/acs.jctc.2c00865
- [49] N. Goel, S. Gupta, M. Sadhukhan and B.M. Deb, *Mol. Phys.* **118** (12), e1676930 (2019). doi:10.1080/00268976.2019.1676930
- [50] H. Hosoda, H. Mori, N. Sogoshi, A. Nagasawa and S. Nakabayashi, *J. Phys. Chem. A* **108** (9), 1461–1464 (2004). doi:10.1021/jp0310145
- [51] E.J.L. Toledo, T.C. Ramalho and Z.M. Magriotis, *J. Mol. Struct.* **888** (1–3), 409–415 (2008). doi:10.1016/j.molstruc.2008.01.010
- [52] R. Cai, H. Yang, J. He and W. Zhu, *J. Mol. Struct.* **938** (1–3), 15–19 (2009). doi:10.1016/j.molstruc.2009.08.037
- [53] K.T. Chang and C.I. Weng, *J. Appl. Phys.* **100** (4), 043917 (2006). doi:10.1063/1.2335971
- [54] E.J.L. Toledo and T.C. Ramalho, *Mol. Simul.* **47** (14), 1159–1167 (2021). doi:10.1080/08927022.2021.1957883
- [55] L. Zhao, K. Ma and Z. Yang, *Int. J. Mol. Sci.* **16** (12), 8454–8489 (2015). doi:10.3390/ijms16048454
- [56] M. Ramos, I. Alkorta, J. Elguero, N.S. Golubev, G.S. Denisov, H. Benedict and H.H. Limbach, *J. Phys. Chem. A* **101** (50), 9791–9800 (1997). doi:10.1021/jp972586q
- [57] S.J. Suresh, A.V. Satish and A. Choudhary, *J. Chem. Phys.* **124** (7), 074506 (2006). doi:10.1063/1.2162888
- [58] R.S. Mulliken, *J. Chem. Phys.* **2** (11), 782–793 (1934). doi:10.1063/1.1749394
- [59] J.E. Huheey and J.C. Watts, *Inorg. Chem.* **10** (7), 1553–1554 (1971). doi:10.1021/ic50101a058
- [60] J.E. Huheey, *J. Org. Chem.* **36** (1), 204–205 (1971). doi:10.1021/jo00800a044
- [61] J.E. Huheey, E.A. Keiter and R.L. Keiter, *Inorganic Chemistry: Principles of Structure and Reactivity* (Harper-Collins College Publishers, New York, 1993).
- [62] E.R. Johnson, S. Keinan, P. Mori-Sánchez, J. Contreras-García, A.J. Cohen and W. Yang, *J. Am. Chem. Soc.* **132** (18), 6498–6506 (2010). doi:10.1021/ja100936w
- [63] R.G. Parr, R.A. Donnelly, M. Levy and W.E. Palke, *J. Chem. Phys.* **68** (8), 3801–3807 (1978). doi:10.1063/1.436185
- [64] R.P. Iczkowski and J.L. Margrave, *J. Am. Chem. Soc.* **83** (17), 3547–3551 (1961). doi:10.1021/ja01478a001
- [65] R.G. Parr and R.G. Pearson, *J. Am. Chem. Soc.* **105** (26), 7512–7516 (1983). doi:10.1021/ja00364a005
- [66] R.G. Pearson, *Chemical Hardness* (Wiley-VCH, Weinheim, Germany, 1997).
- [67] R.G. Parr and W. Yang, *J. Am. Chem. Soc.* **106** (14), 4049–4050 (1984). doi:10.1021/ja00326a036
- [68] P. Geerlings, S. Fias, Z. Boisdenghien and F. De Proft, *Chem. Soc. Rev.* **43** (14), 4989 (2014). doi:10.1039/c3cs60456j
- [69] R.T. Sanderson, *Science* **114** (2973), 670–672 (1951). doi:10.1126/science.114.2973.670
- [70] R.T. Sanderson, *Chemical Bonds and Bond Energy* (Academic Press, New York, 1976).
- [71] R.G. Pearson, *J. Chem. Educ.* **64** (7), 561 (1987). doi:10.1021/ed064p561
- [72] R. Ditchfield, *Mol. Phys.* **27** (4), 789–807 (1974). doi:10.1080/00268977400100711
- [73] T.J.P. Irons, J. Zemen and A.M. Teale, *J. Chem. Theory Comput.* **13** (8), 3636–3649 (2017). doi:10.1021/acs.jctc.7b00540
- [74] E.I. Tellgren, S.S. Reine and T. Helgaker, *Phys. Chem. Chem. Phys.* **14** (26), 9492 (2012). doi:10.1039/c2cp40965h
- [75] S. Stopkowicz, J. Gauss, K.K. Lange, E.I. Tellgren and T. Helgaker, *J. Chem. Phys.* **143** (7), 074110 (2015). doi:10.1063/1.4928056
- [76] F. Hampe and S. Stopkowicz, *J. Chem. Phys.* **146** (15), 154105 (2017). doi:10.1063/1.4979624
- [77] G. Vignale and M. Rasolt, *Phys. Rev. Lett.* **59** (20), 2360–2363 (1987). doi:10.1103/PhysRevLett.59.2360
- [78] E.I. Tellgren, S. Kvaal, E. Sagvolden, U. Ekström, A.M. Teale and T. Helgaker, *Phys. Rev. A* **86** (6), 062506 (2012). doi:10.1103/PhysRevA.86.062506
- [79] J. Simons and P. Jørgensen, *Int. J. Quantum Chem.* **25** (6), 1135–1150 (1984). doi:10.1002/qua.v25:6

- [80] M. Aschi, R. Spezia, A.D. Nola and A. Amadei, *Chem. Phys. Lett.* **344** (3-4), 374–380 (2001). doi:10.1016/S009-2614(01)00638-8
- [81] C.J. Grayce and R.A. Harris, *Phys. Rev. A* **50** (4), 3089–3095 (1994). doi:10.1103/PhysRevA.50.3089
- [82] F.R. Salsbury and R.A. Harris, *J. Chem. Phys.* **107** (18), 7350–7359 (1997). doi:10.1063/1.475165
- [83] E.H. Lieb, *Int. J. Quantum Chem.* **24** (3), 243–277 (1983). doi:10.1002/(ISSN)1097-461X
- [84] S. Kvaal, A. Laestadius, E. Tellgren and T. Helgaker, *J. Phys. Chem. Lett.* **12** (5), 1421–1425 (2021). doi:10.1021/acs.jpcclett.0c03422
- [85] W. Kohn and L.J. Sham, *Phys. Rev.* **140** (4A), A1133–A1138 (1965). doi:10.1103/PhysRev.140.A1133
- [86] S. Reimann, A. Borgoo, J. Austad, E.I. Tellgren, A.M. Teale, T. Helgaker and S. Stopkiewicz, *Mol. Phys.* **117** (1), 97–109 (2018). doi:10.1080/00268976.2018.1495849
- [87] J. Tao, J.P. Perdew, V.N. Staroverov and G.E. Scuseria, *Phys. Rev. Lett.* **91** (14), 146401 (2003). doi:10.1103/PhysRevLett.91.146401
- [88] J.W. Furness, J. Verbeke, E.I. Tellgren, S. Stopkiewicz, U. Ekström, T. Helgaker and A.M. Teale, *J. Chem. Theory Comput.* **11** (9), 4169–4181 (2015). doi:10.1021/acs.jctc.5b00535
- [89] J.F. Dobson, *J. Chem. Phys.* **98** (11), 8870–8872 (1993). doi:10.1063/1.464444
- [90] A.D. Becke, *Can. J. Chem.* **74** (6), 995–997 (1996). doi:10.1139/v96-110
- [91] J.E. Bates and F. Furche, *J. Chem. Phys.* **137** (16), 164105 (2012). doi:10.1063/1.4759080
- [92] T.H. Dunning, *J. Chem. Phys.* **90** (2), 1007–1023 (1989). doi:10.1063/1.456153
- [93] A.K. Wilson, D.E. Woon, K.A. Peterson and T.H. Dunning, *J. Chem. Phys.* **110** (16), 7667–7676 (1999). doi:10.1063/1.478678
- [94] G.L. Stoychev, A.A. Auer and F. Neese, *J. Chem. Theory Comput.* **13** (2), 554–562 (2017). doi:10.1021/acs.jctc.6b01041
- [95] R.S. Mulliken, *J. Chem. Phys.* **23** (10), 1833–1840 (1955). doi:10.1063/1.1740588
- [96] M.J. Pemberton, T.J.P. Irons, T. Helgaker and A.M. Teale, *J. Chem. Phys.* **156** (20), 204113 (2022). doi:10.1063/5.0092520
- [97] D.R. Lide, editor, *CRC Handbook of Chemistry and Physics*, 7th ed. (CRC Press, Inc., Boca Raton, 1994).
- [98] A.J. Ceulemans, *Group Theory Applied to Chemistry* (Springer, Dordrecht, 2013).
- [99] A. Pausch, M. Gebele and W. Klopper, *J. Chem. Phys.* **155** (20), 201101 (2021). doi:10.1063/5.0069859
- [100] P. Lazzeretti, M. Malagoli and R. Zanasi, in *Nuclear Magnetic Shieldings and Molecular Structure*, edited by J. A. Tossell (Springer Science+Business Media, B.V., Maryland, 1993), p. 163.
- [101] S. Pelloni and P. Lazzeretti, *Int. J. Quantum Chem.* **111** (2), 356–367 (2011). doi:10.1002/qua.22658
- [102] T.J.P. Irons, L. Spence, G. David, B.T. Speake, T. Helgaker and A.M. Teale, *J. Phys. Chem. A* **124** (7), 1321–1333 (2020). doi:10.1021/acs.jpca.9b10833
- [103] R.G. Parr and L.J. Bartolotti, *J. Am. Chem. Soc.* **104** (14), 3801–3803 (1982). doi:10.1021/ja00378a004
- [104] Y. Yafet, R. Keyes and E. Adams, *J. Phys. Chem. Solids* **1** (3), 137–142 (1956). doi:10.1016/0022-3697(56)90020-8
- [105] R.H. Garstang, *Rep. Progr. Phys.* **40** (2), 105–154 (1977). doi:10.1088/0034-4885/40/2/001
- [106] G. Pagola, M. Caputo, M. Ferraro and P. Lazzeretti, *Chem. Phys. Lett.* **400** (1-3), 133–138 (2004). doi:10.1016/j.cplett.2004.10.057
- [107] J.A. Weil and J.R. Bolton, *Electron Paramagnetic Resonance*, 2nd ed. (John Wiley & Sons, Inc., Hoboken, New Jersey, 2007).
- [108] E.I. Tellgren, A. Laestadius, T. Helgaker, S. Kvaal and A.M. Teale, *J. Chem. Phys.* **148** (2), 024101 (2018). doi:10.1063/1.5007300
- [109] H. Fukutome, *Int. J. Quantum Chem.* **20** (5), 955–1065 (1981). doi:10.1002/(ISSN)1097-461X

Appendix. Symmetry of molecules in external magnetic fields

While the layperson approach to determining the full symmetry of a molecular system under an external magnetic field presented in Section 3.1 should suffice in many cases, the avid readers with a keen eye for the subtleties of the time-reversal symmetry will inevitably find such an approach rather unsatisfying. Therefore, in this Appendix, a more formal discussion on the symmetry of molecules in external magnetic fields will be presented.

For an N -electron system in an *external* magnetic field $\mathbf{B}(\mathbf{r}) = \nabla \times \mathbf{A}(\mathbf{r})$ where $\mathbf{A}(\mathbf{r})$ denotes the *external* magnetic vector potential, the Schrödinger–Pauli Hamiltonian describing this system is given in atomic units by [107, 108]

$$\hat{\mathcal{H}} = \hat{\mathcal{H}}_0(v_{\text{ext}}) + \sum_{k=1}^N \mathbf{A}(\mathbf{r}_k) \cdot \hat{\mathbf{p}}_k + \frac{g_s}{2} \sum_{k=1}^N \mathbf{B}(\mathbf{r}_k) \cdot \hat{\mathbf{s}}_k + \frac{1}{2} \sum_{k=1}^N A^2(\mathbf{r}_k), \quad (\text{A1})$$

where $\hat{\mathcal{H}}_0$ is the zero-field Hamiltonian that depends on the multiplicative external potential v_{ext} , $\hat{\mathbf{p}}_k$ is the canonical momentum operator for the k^{th} electron, g_s the electron spin g -factor, and $\hat{\mathbf{s}}_k$ the spin angular momentum operator for the k^{th} electron. This is essentially equivalent to the electronic Hamiltonian introduced in Equation (12), but written in a more compact and general form to facilitate the symmetry discussion to follow. The symmetry of this system is governed by its symmetry group \mathcal{M} which comprises all transformations \hat{t} that leave $\hat{\mathcal{H}}$ invariant, *i.e.* $\hat{t}\hat{\mathcal{H}}\hat{t}^{-1} = \hat{\mathcal{H}}$. Clearly, \mathcal{M} is the intersection of the symmetry groups of the four constituent terms in Equation (A1) which shall now be discussed in turn.

A.1 The zero-field Hamiltonian

Consider first the zero-field Hamiltonian:

$$\hat{\mathcal{H}}_0(v_{\text{ext}}) = \frac{1}{2} \sum_{k=1}^N \hat{p}_k^2 + \sum_{k=1}^N v_{\text{ext}}(\mathbf{r}_k) + \frac{1}{2} \sum_{k \neq l}^N \frac{1}{|\mathbf{r}_k - \mathbf{r}_l|}.$$

As both the kinetic energy term and the two-electron interaction term are invariant under all spatial proper and improper rotations, the symmetry group of $\hat{\mathcal{H}}_0$ is determined exclusively by the external potential v_{ext} which arises from the spatial geometric arrangement of the nuclear framework. We thus let

\mathcal{G} be the largest subgroup of the full orthogonal transformation group in three dimensions, $\mathbf{O}(3)$, under which v_{ext} , and hence $\hat{\mathcal{H}}_0$, is invariant. \mathcal{G} is commonly called the *point group* of the system, but in anticipation of the discussion below, we shall, however, refer to \mathcal{G} as the system's *spatial unitary symmetry group* to make clear the fact that \mathcal{G} only contains unitary symmetry transformations that leave the spatial nuclear framework unchanged. The absence of spin-dependent and magnetic-field-dependent terms in $\hat{\mathcal{H}}_0$ means that $\hat{\mathcal{H}}_0$ is also invariant under the action of the time reversal operator $\hat{\theta}$. Therefore, the full symmetry group for $\hat{\mathcal{H}}_0$ is given by

$$\mathcal{G} + \hat{\theta}\mathcal{G} \quad (\text{A2})$$

where the '+' denotes a disjoint union.

A.2 Terms including the magnetic vector potential

Consider next the second term in Equation (A1) which, for each k^{th} electron in the system, describes the interaction between its canonical momentum $\hat{\mathbf{p}}_k$ and the external magnetic vector potential $\mathbf{A}(\mathbf{r}_k)$. As this term involves two factors, one internal to the system (the canonical momenta of the electrons), and one external (the magnetic vector potential), care must be taken when applying transformation operations on it. In particular, it shall be agreed that transformation operations only affect the system which consists of the nuclei and the electrons, but not external parameters that arise from sources lying outside the system. This means that $\mathbf{A}(\mathbf{r}_k)$ shall be untouched by the action of a transformation \hat{t} while only $\hat{\mathbf{p}}_k$ is affected. In other words,

$$\hat{t} [\mathbf{A}(\mathbf{r}_k) \cdot \hat{\mathbf{p}}_k] \hat{t}^{-1} = \mathbf{A}(\mathbf{r}_k) \cdot (\hat{t}\hat{\mathbf{p}}_k\hat{t}^{-1}). \quad (\text{A3})$$

First, let $\hat{t} = \hat{u} \in \mathbf{O}(3)$ be an orthogonal three-dimensional transformation operator with representation matrix \mathbf{U} in the orthonormal Cartesian basis $\{\mathbf{i}, \mathbf{j}, \mathbf{k}\}$. To see which transformations leave $\mathbf{A}(\mathbf{r}_k) \cdot \hat{\mathbf{p}}_k$ unchanged, we write Equation (A3) in a more helpful form:

$$\begin{aligned} & \mathbf{A}(\mathbf{r}_k) \cdot (\hat{u}\hat{\mathbf{p}}_k\hat{u}^{-1}) \\ &= \sum_{\mu} A_{\mu}(\mathbf{r}_k) \hat{u}\hat{p}_{k\mu}\hat{u}^{-1} = \sum_{\mu\nu} A_{\mu}(\mathbf{r}_k) U_{\mu\nu} \hat{p}_{k\nu} \\ &= \sum_{\nu} \left[\sum_{\mu} U_{\mu\nu} A_{\mu}(\mathbf{r}_k) \right] \hat{p}_{k\nu} = [\mathbf{U}^{-1}\mathbf{A}(\mathbf{r}_k)] \cdot \hat{\mathbf{p}}_k, \end{aligned} \quad (\text{A4})$$

where $\mu, \nu \in \{x, y, z\}$ and the fact that $\hat{\mathbf{p}}_k$ is a polar vector has been utilised. Imposing the invariance $[\mathbf{U}^{-1}\mathbf{A}(\mathbf{r}_k)] \cdot \hat{\mathbf{p}}_k = \mathbf{A}(\mathbf{r}_k) \cdot \hat{\mathbf{p}}_k$ at all points \mathbf{r}_k in \mathbb{R}^3 gives

$$\mathbf{U}^{-1}\mathbf{A}(\mathbf{r}_k) = \mathbf{A}(\mathbf{r}_k) \iff \mathbf{A}(\mathbf{r}_k) = \mathbf{U}\mathbf{A}(\mathbf{r}_k), \quad (\text{A5})$$

which states that \hat{u} must be an orthogonal transformation in three dimensions that, if it acted on the external magnetic vector potential $\mathbf{A}(\mathbf{r}_k)$ (which is a polar vector), would leave it everywhere unchanged. Since $\mathbf{B}(\mathbf{r}_k) = \nabla \times \mathbf{A}(\mathbf{r}_k)$, this condition is equivalent to the condition that \hat{u} would also leave $\mathbf{B}(\mathbf{r}_k)$ invariant if it were to act on $\mathbf{B}(\mathbf{r}_k)$ [cf. Equation (A8) below]. It is important to note the subjunctive used deliberately in the two condition statements because, as shown clearly in Equation (A3), these operations do not actually act on external parameters when transforming the Hamiltonian. Nevertheless, these conditions essentially form the basis for the layperson

approach presented in Section 3.1 and allow one to deduce that, for a uniform external magnetic field described by an axial vector \mathbf{B} , the orthogonal transformations in three dimensions that would map \mathbf{B} onto itself and that leave $\mathbf{A}(\mathbf{r}_k) \cdot \hat{\mathbf{p}}_k$ invariant form an infinite group commonly known as $\mathcal{C}_{\infty h}$ [98, 99].

Next, take $\hat{t} = \hat{\theta}$ to be the antiunitary time-reversal operator. As $\hat{\mathbf{p}}_k = -i\nabla_k$ is purely imaginary, it follows that $\hat{\theta}\hat{\mathbf{p}}_k\hat{\theta}^{-1} = -\hat{\mathbf{p}}_k$. Time reversal is thus not a symmetry transformation of $\mathbf{A}(\mathbf{r}_k) \cdot \hat{\mathbf{p}}_k$. However, in the light of the discussion in the above paragraph, if we take $\hat{t} = \hat{\theta}\hat{u}$ instead where $\hat{u} \in \mathbf{O}(3)$ reverses the direction of $\mathbf{A}(\mathbf{r}_k)$ [and hence $\mathbf{B}(\mathbf{r}_k)$] and thus introduces a sign change to $\mathbf{A}(\mathbf{r}_k) \cdot \hat{\mathbf{p}}_k$ which is then annihilated by $\hat{\theta}$, then the antiunitary product $\hat{\theta}\hat{u}$ indeed keeps $\mathbf{A}(\mathbf{r}_k) \cdot \hat{\mathbf{p}}_k$ invariant. For a uniform magnetic field \mathbf{B} , such unitary operations \hat{u} form an infinite set of two-fold rotations about axes perpendicular to \mathbf{B} (collectively denoted $\infty\mathcal{C}_2^{\perp}$) and the infinite set of reflections in planes which contain \mathbf{B} (collectively denoted $\infty\sigma_v$). The full symmetry group of the term $\mathbf{A}(\mathbf{r}_k) \cdot \hat{\mathbf{p}}_k$ is thus

$$\mathcal{C}_{\infty h} + \hat{\theta}\{\infty\mathcal{C}_2^{\perp}, \infty\sigma_v\}. \quad (\text{A6})$$

It is then trivial to see that, as the last term in Equation (A1) involves only the squared magnitude of the external vector potential, it remains invariant under all spatial transformations and time reversal which act only on the system. Its full symmetry group is therefore

$$\mathbf{O}(3) + \hat{\theta}\mathbf{O}(3). \quad (\text{A7})$$

A.3 The spin Zeeman interaction term

Following the same argument in the paragraph preceding Equation (A3), the transformation law for the third term in Equation (A1) is given by

$$\hat{t} [\mathbf{B}(\mathbf{r}_k) \cdot \hat{\mathbf{s}}_k] \hat{t}^{-1} = \mathbf{B}(\mathbf{r}_k) \cdot (\hat{t}\hat{\mathbf{s}}_k\hat{t}^{-1}).$$

If $\hat{t} = \hat{u} \in \mathbf{O}(3)$, then

$$\begin{aligned} & \mathbf{B}(\mathbf{r}_k) \cdot (\hat{u}\hat{\mathbf{s}}_k\hat{u}^{-1}) \\ &= \sum_{\mu} B_{\mu}(\mathbf{r}_k) \hat{u}\hat{s}_{k\mu}\hat{u}^{-1} = \sum_{\mu\nu} B_{\mu}(\mathbf{r}_k) |\mathbf{U}| U_{\mu\nu} \hat{s}_{k\nu} \\ &= \sum_{\nu} \left[\sum_{\mu} |\mathbf{U}| U_{\mu\nu} B_{\mu}(\mathbf{r}_k) \right] \hat{s}_{k\nu} = [|\mathbf{U}|\mathbf{U}^{-1}\mathbf{B}(\mathbf{r}_k)] \cdot \hat{\mathbf{s}}_k, \end{aligned}$$

where the determinant $|\mathbf{U}|$ appears because the spin angular momentum operator is an axial vector. This yields an invariance condition identical to that in Equation (A5) but expressed in terms of the axial magnetic field:

$$|\mathbf{U}|\mathbf{U}^{-1}\mathbf{B}(\mathbf{r}_k) = \mathbf{B}(\mathbf{r}_k) \iff \mathbf{B}(\mathbf{r}_k) = |\mathbf{U}|\mathbf{U}\mathbf{B}(\mathbf{r}_k), \quad (\text{A8})$$

where the fact that $|\mathbf{U}| = \pm 1$ has been exploited. If $\hat{t} = \hat{\theta}$, then it is well-known [109] that $\hat{\theta}\hat{\mathbf{s}}_k\hat{\theta}^{-1} = -\hat{\mathbf{s}}_k$, and so the sign of $\mathbf{B}(\mathbf{r}_k) \cdot \hat{\mathbf{s}}_k$ is flipped by time reversal. For a uniform magnetic field, the full symmetry group of $\mathbf{B} \cdot \hat{\mathbf{s}}_k$ is thus identical to that of $\mathbf{A}(\mathbf{r}_k) \cdot \hat{\mathbf{p}}_k$ in Equation (A6).

A.4 Overall molecular symmetry in external uniform magnetic fields

The full symmetry group \mathcal{M} of the Hamiltonian $\hat{\mathcal{H}}$ in Equation (A1) for a uniform external magnetic field \mathbf{B} is given by the

intersection of the symmetry groups in Equations (A2), (A6), and (A7):

$$\begin{aligned}\mathcal{M} &= (\mathcal{G} + \hat{\theta}\mathcal{G}) \cap (\mathcal{C}_{\infty h} + \hat{\theta}\{\infty C_2^\perp, \infty\sigma_v\}) \\ &\quad \cap (\mathbf{O}(3) + \hat{\theta}\mathbf{O}(3)) \\ &= (\mathcal{G} \cap \mathcal{C}_{\infty h}) + \hat{\theta}(\mathcal{G} \cap \{\infty C_2^\perp, \infty\sigma_v\}).\end{aligned}$$

Let $\mathcal{H} = \mathcal{G} \cap \mathcal{C}_{\infty h}$ be the unitary part of \mathcal{M} . Since \mathcal{G} and $\mathcal{C}_{\infty h}$ are both groups, it is trivial to show that \mathcal{H} must also be a group, and hence a subgroup of \mathcal{M} . We thus refer to \mathcal{H} as the *magnetic unitary symmetry subgroup* of the system.

The antiunitary part of \mathcal{M} is less straightforward. There are two possibilities for the intersection $\mathcal{G} \cap \{\infty C_2^\perp, \infty\sigma_v\}$:

- (1) $\mathcal{G} \cap \{\infty C_2^\perp, \infty\sigma_v\}$ is empty, which means that the system's spatial unitary symmetry group \mathcal{G} contains no operations that would reverse the direction of \mathbf{B} . We then have

$$\mathcal{M} = \mathcal{H}$$

and the full symmetry group of the system is entirely unitary.

- (2) $\mathcal{G} \cap \{\infty C_2^\perp, \infty\sigma_v\}$ is not empty, which means \mathcal{G} contains operations that would reverse the direction of \mathbf{B} . \mathcal{H} is now

a proper subgroup of \mathcal{M} , and by Lagrange's theorem, the order of \mathcal{H} must divide the order of \mathcal{M} . To determine the index of \mathcal{H} in \mathcal{M} , let \hat{u} and \hat{v} be two elements in $\mathcal{G} \cap \{\infty C_2^\perp, \infty\sigma_v\}$. Assume, for the sake of contradiction, that the two left cosets $\hat{\theta}\hat{u}\mathcal{H}$ and $\hat{\theta}\hat{v}\mathcal{H}$ are distinct. This means that

$$\forall h \in \mathcal{H} \quad \hat{\theta}\hat{u}h \notin \hat{\theta}\hat{v}\mathcal{H},$$

which implies $\hat{v}^{-1}\hat{u} \notin \mathcal{H}$ when h is chosen to be the identity. But as both \hat{v}^{-1} and \hat{u} must lie in \mathcal{G} , and as their product must preserve the direction of \mathbf{B} , that $\hat{v}^{-1}\hat{u} \notin \mathcal{H}$ is a contradiction, and so $\hat{\theta}\hat{u}\mathcal{H}$ is unique for any $\hat{u} \in \mathcal{G} \cap \{\infty C_2^\perp, \infty\sigma_v\}$. Hence, \mathcal{H} must be a subgroup of index 2 in \mathcal{M} . It is then easy to see that \mathcal{H} must also be normal in \mathcal{M} . We thus write

$$\mathcal{M} = \mathcal{H} + \hat{\theta}\hat{u}\mathcal{H}$$

for some $\hat{u} \in \mathcal{G} \cap \{\infty C_2^\perp, \infty\sigma_v\}$. The group \mathcal{M} is now no longer unitary but can be isomorphic (although not identical) to a unitary group \mathcal{M}' , in which case we also write [100, 101]

$$\mathcal{M} = \mathcal{M}'(\mathcal{H}).$$

We refer to \mathcal{M} as the full *magnetic symmetry group* of the system.